Synthesis and Spectroscopic Characterization of Pyrrolidyl and Piperidyl Dithioformate Derivatives of Dimethyltellurium(IV) Compounds. Crystal Structures of $Me_2Te[S_2CN(CH_2)_3CH_2]_2$, $Me_2Te[S_2CN(CH_2)_4CH_2]_2$, $Me_2Te\{[S_2CN(CH_2)_3CH_2][S_2CN(CH_2)_4CH_2]\}$, $Me_2TeCl[S_2CN(CH_2)_3CH_2]$, $Me_2TeBr[S_2CN(CH_2)_3CH_2]$, $Me_2TeI[S_2CN(CH_2)_3CH_2]$, $Me_2TeCl[S_2CN(CH_2)_4CH_2]$, and $Me_2TeI[S_2CN(CH_2)_4CH_2]$

John E. Drake* and Jincai Yang

Department of Chemistry and Biochemistry, University of Windsor, Windsor, Ontario, Canada N9B 3P4

Received July 18, 1996[⊗]

Dimethylbis(pyrrolidyl and piperidyl dithioformato)tellurium(IV) compounds and the corresponding halodimethyl compounds, $Me_2TeX[S_2CN(CH_2)_nCH_2]$, where $n = 3$, 4 and X = Cl, Br, and I, have been prepared. The compounds were characterized by elemental analysis and IR, Raman, and multinuclear NMR spectroscopies, including some variable temperature studies. The following crystallize as monoclinic in space group $P2_1/c$ (No. 14). $Me_2Te[S_2CN(CH_2)_3CH_2]_2$ **(1)**: $a = 6.38(1)$ Å, $b = 18.902(7)$ Å, $c = 14.672(6)$ Å, $\beta = 97.73(6)°$ $V = 1752(2)$ Å^3, $Z = 4$, $R = 0.0636$, $R_w = 0.0642$. $Me_2Te\{[S_2CN(CH_2)_3CH_2][S_2CN(CH_2)_4(CH_2)]\}$ **(3)**: $a = 6.55(1)$ Å, $b = 19.716(6)$ Å, $c = 14.900(9)$ Å, $\beta = 95.27(8)°$, $V = 1928(3)$ Å^3, $Z = 4$, $R = 0.0618$, $R_w = 0.0511$. $Me_2TeCl[S_2CN(CH_2)_3CH_2]$ **(4)**: $a = 9.952(3)$ Å, $b = 6.386(3)$ Å, $c = 18.834(3)$ Å, $\beta = 95.32(2)°$, $V = 1191.7(6)$ Å^3, $Z = 4$, $R = 0.0358$, $R_w = 0.0314$. $Me_2TeBr[S_2CN(CH_2)_3CH_2]$ **(5)**: $a = 10.085(4)$ Å, $b = 6.446(4)$ Å, $c = 19.020(5)$ Å, $\beta = 95.08(3)°$, $V = 1231.7(8)$ Å^3, $Z = 4$, $R = 0.0559$, $R_w = 0.0469$. $Me_2TeCl[S_2CN(CH_2)_4CH_2]$ **(7)** is $P2_1/a$ (No. 14) with $a = 9.756(2)$ Å, $b = 11.242(2)$ Å, $c = 12.028(3)$ Å, $\beta = 92.26(3)°$, $V = 1318.2(7)$ Å^3, $Z = 4$, $R = 0.0438$, $R_w = 0.0442$, and $Me_2TeI[S_2CN(CH_2)_4CH_2]$ **(9)** is $P2_1$ (No. 4) with $a = 6.019(3)$ Å, $b = 8.986(4)$ Å, $c = 13.012(2)$ Å, $\beta = 100.61(3)°$, $V = 691.7(6)$ Å^3, $Z = 2$, $R = 0.0364$, $R_w = 0.0305$. $Me_2TeI[S_2CN(CH_2)_3CH_2]$ **(6)** is orthorhombic in *Pbca* (No. 61) with $a = 13.951(6)$ Å, $b = 19.849(8)$ Å, $c = 9.261(4)$ Å, $V = 2564(1)$ Å^3, $Z = 8$, $R = 0.0392$, $R_w = 0.0326$, and $Me_2Te[S_2CN(CH_2)_4CH_2]_2$ **(2)** is triclinic in $P\bar{1}$ (No. 2) with $a = 9.624(2)$ Å, $b = 12.904(3)$ Å, $c = 9.008(2)$ Å, $\alpha = 98.29(2)°$, $\beta = 111.19(2)°$, $\gamma = 99.64(2)°$, $V = 1002.5(4)$ Å^3, $Z = 2$, $R = 0.0504$, $R_w = 0.0454$. The immediate environment about Te is that of a sawhorse structure in which the lone pair is apparently stereochemically active and occupying an equatorial position in a distorted trigonal bipyramid. The second sulfur atom appears also to be in the coordination sphere resulting in the following distorted arrangements about Te: pseudo pentagonal bipyramidal in **1** and **3**, octahedral in **2**, and square pyramidal in **5**, **6**, **7**, and **9**.

Introduction

The importance of supramolecular associations in molecular compounds of tellurium complexes with sulfur ligands has been recently reviewed.[1] Several reports have appeared on organotellurium(IV) derivatives with 1,1-dithio ligands including *O*-alkyl dithiocarbonates[2−7] and *N*,*N*-dialkyl dithiocarbamates.[5−16] We recently reported on dimethyltellurium derivatives of monothio ligands including pyrrolidyl and piperidyl monothioformate derivatives,[17] but unfortunately were only able to obtain structural information on ethyl derivatives. We now report on the synthesis and spectroscopic characterization of dimethyltellurium(IV) pyrrolidyl and piperidyl dithioformates, $Me_2Te[S_2CN(CH_2)_nCH_2]_2$ and $Me_2TeX[S_2CN(CH_2)_nCH_2]$, where $n = 3$, 4 and X = Cl, Br, and I. X-ray crystal structures are reported for $Me_2Te[S_2CN(CH_2)_3CH_2]_2$ **(1)**, $Me_2Te[S_2CN(CH_2)_4CH_2]_2$ **(2)**, $Me_2Te\{[S_2CN(CH_2)_3CH_2][S_2CN(CH_2)_4CH_2]\}$ **(3)**, $Me_2TeCl[S_2CN(CH_2)_3CH_2]$ **(4)**, $Me_2TeBr[S_2CN(CH_2)_3CH_2]$ **(5)**, $Me_2TeI[S_2CN(CH_2)_3CH_2]$ **(6)**, $Me_2TeCl[S_2CN(CH_2)_4CH_2]$ **(7)**, and $Me_2TeI[S_2CN(CH_2)_4CH_2]$ **(9)**.

Experimental Section

Materials. $TeCl_4$ and Me_4Sn were obtained from Aldrich, and $TeBr_4$ and Me_2TeI_2, from Alfa and Organometallics, Inc., respectively; all

* Author to whom correspondence should be addressed. E-mail: ak4@uwindsor.ca.

[⊗] Abstract published in *Advance ACS Abstracts,* March 15, 1997.

(1) Haiduc, I.; King, R. B.; Newton, M. G. *Chem. Rev.* **1994**, *94*, 301.
(2) Bailey, J. H. E.; Drake, J. E.; Khasrou, L. N.; Yang, J. *Inorg. Chem.* **1995**, *34*, 124.
(3) Wieber, M.; Schmidt, E.; Burschka, C. *Z. Anorg. Allg. Chem.* **1985**, *525*, 127.
(4) Singh, A. K.; Basumatary, J. K.; Singh, T. P.; Padmanabhan, B. *J. Organomet. Chem.* **1992**, *424*, 33.
(5) Husebye, S.; Maartmann-Moe, K.; Mikalsen, O. *Acta Chem. Scand.* **1990**, *44*, 464.
(6) Dakternieks, D.; Di Giacomo, R.; Gable, R. W.; Hoskins, B. F. *J. Am. Chem. Soc.* **1988**, *110*, 6753.
(7) Singh, A. K.; Basumatary, J. K. *J. Organomet. Chem.* **1989**, *364*, 73.
(8) Dakternieks, D.; Di Giacomo, R.; Gable, R. W.; Hoskins, B. F. *J. Am. Chem. Soc.* **1988**, *110*, 6762.
(9) Dakternieks, D.; Di Giacomo, R.; Gable, R. W.; Hoskins, B. F. *J. Organomet. Chem.* **1988**, *349*, 305.
(10) Bailey, J. H. E.; Drake, J. E.; Sarkar, A. B.; Wong, M. L. Y. *Can. J. Chem.* **1989**, *67*, 1735.
(11) Bailey, J. H. E.; Drake, J. E.; Wong, M. L. Y. *Can. J. Chem.* **1991**, *69*, 1948.
(12) Drake, J. E.; Wong, M. L. Y. *J. Organomet. Chem.* **1989**, *377*, 43.
(13) Husebye, S.; Maartmann-Moe, K.; Steffenson, W. *Acta Chem. Scand.* **1990**, *44*, 139.
(14) Husebye, S.; Maartmann-Moe, K.; Steffenson, W. *Acta Chem. Scand.* **1990**, *44*, 579.
(15) Bailey, J. H. E.; Drake, J. E. *Can. J. Chem.* **1993**, *71*, 42.
(16) Srivastava, T. N.; Srivastava, R. C.; Bhargava, A. *Indian J. Chem.* **1979**, *18A*, 236.
(17) Drake, J. E.; Khasrou, L. N.; Mislankar, A. G.; Ratnani, R. *Inorg. Chem.* **1994**, *33*, 6154.

S0020-1669(96)00845-2 CCC: $14.00

starting materials were used as supplied. Me_2TeCl_2 and Me_2TeBr_2 were prepared by the adaption of the method described in the literature for the preparation of Ph_2TeCl_2[18] by the reaction of $TeCl_4$ or $TeBr_4$ with Me_4Sn in toluene at 60 °C under reflux for 4 h. Sodium salts of pyrrolidyl and piperidyl dithioformates[19] were prepared by literature methods. All solvents were dried and distilled prior to use and all reactions were carried out under anhydrous conditions. Elemental analyses were performed at Guelph Chemical Laboratories, Guelph, Ontario, Canada.

Preparation of Dimethylbis(pyrrolidyl dithioformato)- and dimethylbis(piperidyl dithioformato)tellurium(IV), $Me_2Te[S_2CN(CH_2)_3CH_2]_2$ (1) and $Me_2Te[S_2CN(CH_2)_4CH_2]_2$ (2). Typically, dimethyltellurium dichloride (0.150 g, 0.656 mmol) and the sodium salt of pyrrolidyl dithioformate (0.250 g, 1.479 mmol) were placed in a flask followed by the addition of dichloromethane or toluene (10 mL). The mixture was stirred at room temperature for 2 h before being filtered to remove NaCl and unreacted materials. The solvent was allowed to evaporate under vacuum to yield a yellow solid. $Me_2Te[S_2CN(CH_2)_3CH_2]_2$ (**1**) was recrystallized from a dichloromethane/*n*-hexane or toluene/*n*-hexane mixture held at 5 °C to give yellow crystals: 0.255 g, yield 86%; mp 152 °C. Similarly, dimethyltellurium dichloride (0.083 g, 0.363 mmol) and the sodium salt of piperidyl dithioformate (0.150 g, 0.820 mmol) formed $Me_2Te[S_2CN(CH_2)_4CH_2]_2$ (**2**): 0.154 g, yield 89%; mp 140 °C. Anal. Calcd for $C_{14}H_{26}N_2S_4Te$: C, 35.18; H, 5.44; N, 5.86. Found: C, 35.03; H, 5.63; N, 5.78.

Preparation of Dimethyl(piperidyl dithioformato)(pyrrolidyldithioformato)tellurium(IV), $Me_2Te\{[S_2CN(CH_2)_3CH_2][S_2CN(CH_2)_4CH_2]\}$ (3). Typically, dimethyltellurium dichloride (0.116 g, 0.507 mmol) and the sodium salt of piperidyl dithioformate (0.093 g, 0.507 mmol) were placed in a flask followed by the addition of dichloromethane (10 mL). The mixture was stirred at room temperature for 30 min before the sodium salt of pyrrolidyl dithioformate (0.086 g, 0.507 mmol) was added, and the stirring continued for a further 1.5 h before the mixture was filtered to remove NaCl and unreacted materials. The solvent was allowed to evaporate under vacuum to yield a yellow solid. $Me_2Te\{[S_2CN(CH_2)_3CH_2][S_2CN(CH_2)_4CH_2]\}$ (**3**) was recrystallized from a CH_2Cl_2/*n*-hexane mixture held at 5 °C to give yellow crystals: 0.204 g, yield 87%; mp 140 °C. Anal. Calcd for $C_{13}H_{24}N_2S_4Te$: C, 33.65; H, 5.18; N, 6.04. Found: C, 32.48; H, 5.21; N, 5.60.

Preparation of Chlorodimethyl(pyrrolidyl and piperidyl dithioformato)tellurium(IV), $Me_2TeCl[S_2CN(CH_2)_3CH_2]$ (4) and $Me_2TeCl[S_2CN(CH_2)_4CH_2]$ (7). Typically, dimethyltellurium dichloride (0.152 g, 0.663 mmol) and the sodium salt of pyrrolidyl dithioformate (0.112 g, 0.663 mmol) were placed in a flask followed by the addition of dichloromethane or toluene (10 mL). The mixture was stirred at room temperature for 2 h before being filtered to remove NaCl and unreacted materials. The solvent was allowed to evaporate under vacuum to yield a pale-yellow solid. $Me_2TeCl[S_2CN(CH_2)_3CH_2]_2$ (**4**) was recrystallized from a dichloromethane/*n*-hexane mixture held at 5 °C to give colorless crystals: 0.197 g, yield 88%; dec 115 °C. Similarly, dimethyltellurium dichloride (0.120 g, 0.525 mmol) and the sodium salt of piperidyl dithioformate (0.096 g, 0.525 mmol) formed $Me_2TeCl[S_2CN(CH_2)_4CH_2]_2$ (**7**) as colorless crystals: 0.165 g, yield 89%; dec 140 °C. Anal. Calcd for $C_7H_{16}NS_2ClTe$: C, 27.19; H, 4.53; N, 3.96. Found: C, 27.23; H, 4.30; N, 3.87.

Preparation of Bromodimethyl(pyrrolidyl and piperidyl dithioformato)tellurium(IV), $Me_2TeBr[S_2CN(CH_2)_3CH_2]$ (5) and $Me_2TeBr[S_2CN(CH_2)_4CH_2]$ (8). Typically, dimethyltellurium dibromide (0.078 g, 0.245 mmol) and the sodium salt of pyrrolidyl dithioformate (0.042 g, 0.245 mmol) were placed in a flask followed by the addition of dichloromethane or toluene (10 mL). The mixture was stirred at room temperature for 2 h before being filtered to remove NaBr and unreacted materials. The solvent was allowed to evaporate under vacuum to yield a pale-yellow solid. $Me_2TeBr[S_2CN(CH_2)_3CH_2]_2$ (**5**) was recrystallized from a dichloromethane/*n*-hexane mixture held at 5 °C to give pale-yellow crystals: 0.078 g, yield 83%; dec 130 °C. Anal. Calcd for $C_6H_{14}NS_2BrTe$: C, 21.90; H, 3.65; N, 3.65. Found: C, 21.90; H, 3.57; N, 3.77. Similarly, dimethyltellurium dibromide (0.800 g, 0.250 mmol) and the sodium salt of piperidyl dithioformate (0.046 g, 0.250 mmol) formed $Me_2TeBr[S_2CN(CH_2)_4CH_2]_2$ (**8**) as pale-yellow crystals: 0.083 g, yield 83%; dec 90 °C.

Preparation of Iododimethyl(pyrrolidyl and piperidyl dithioformato)tellurium(IV), $Me_2TeI[S_2CN(CH_2)_3CH_2]$ (6) and $Me_2TeI[S_2CN(CH_2)_4CH_2]$ (9). Typically, dimethyltellurium diiodide (0.230 g, 0.559 mmol) and the sodium salt of pyrrolidyl dithioformate (0.094 g, 0.559 mmol) were placed in a flask followed by the addition of dichloromethane or toluene (10 mL). The mixture was stirred at room temperature for 2 h before being filtered to remove NaI and unreacted materials. The solvent was allowed to evaporate under vacuum to yield a yellow solid. $Me_2TeI[S_2CN(CH_2)_3CH_2]_2$ (**6**) was recrystallized from a dichloromethane/*n*-hexane mixture held at 5 °C to give yellow crystals: 0.215 g, yield 89%; dec 110 °C. Similarly, dimethyltellurium diiodide (0.192 g, 0.467 mmol) and the sodium salt of piperidyl dithioformate (0.085 g, 0.467 mmol) formed $Me_2TeI[S_2CN(CH_2)_4CH_2]_2$ (**9**): 0.181 g, yield 87%; dec 110 °C. Anal. Calcd for $C_7H_{16}NS_2ITe$: C, 21.60; H, 3.60; N, 3.15. Found: C, 21.66; H, 3.66; N, 3.06.

Physical Measurements. The infrared spectra were recorded on a Nicolet 5DX FT spectrometer as KBr pellets and far-infrared spectra on a Bomem IR spectrometer between polyethylene films. The Raman spectra were recorded on a Spectra-Physics 164 spectrometer using the 5145 Å exciting line of an argon ion laser in sealed glass capillaries. The ^1H and $^{13}C\{H\}$ NMR spectra were recorded on a Bruker 300 FT/NMR spectrometer at 300.133 and 75.471 MHz, respectively, in $CDCl_3$ using Me_4Si as internal standard. The ^{125}Te NMR spectra were recorded on a Bruker 200 FT/NMR spectrometer in $CDCl_3$ using Me_2Te as external standard. All NMR spectra were run at ambient temperature, with the exception of the routine VT NMR studies, and under standard operating conditions. The melting points were determined on a Fisher-Johns apparatus.

X-ray Crystallographic Analysis. Yellow block-shaped crystals of $Me_2Te[S_2CN(CH_2)_3CH_2]_2$ **(1)**, $Me_2Te\{[S_2CN(CH_2)_3CH_2][S_2CN(CH_2)_4CH_2]\}$ **(3)**, $Me_2TeCl[S_2CN(CH_2)_3CH_2]$ **(4)**, $Me_2TeBr[S_2CN(CH_2)_3CH_2]$ **(5)**, $Me_2TeI[S_2CN(CH_2)_3CH_2]$ **(6)**, and $Me_2TeI[S_2CN(CH_2)_4CH_2]$ **(9)** and a colorless block crystal of $Me_2TeCl[S_2CN(CH_2)_4CH_2]$ **(7)** were mounted on glass fibers and sealed with epoxy glue. A yellow block crystal of $Me_2Te[S_2N(CH_2)_4CH_2]_2$ **(2)** was mounted in a sealed thin-walled glass capillary. Data were collected on a Rigaku AFC6S diffractometer, with graphite-monochromated Mo Kα radiation operating at 50 kV and 35 mA.

Cell constants and an orientation matrix for data collection, obtained from a least-squares refinement using the setting angles of up to 24 carefully centered reflections in the overall range $8.36 < 2\theta < 20.64$, corresponded to monoclinic cells (for **1**, **3**, **4**, **5**, **7**, and **9**), and triclinic and orthorhombic cells (for **2** and **6**, respectively) whose dimensions are given in Table 1. On the basis of the systematic absences (*h*0*l*, $l = 2n + 1$; 0*k*0, $k = 2n + 1$ for **1**, **3**, **4**, and **5**), (0*kl*, $k = 2n + 1$; *h*0*l*, $l = 2n + 1$; *hk*0, $h = 2n + 1$ for **6**), (*h*0*l*, $h = 2n + 1$; 0*k*0, $k = 2n + 1$ for **7**), and (0*k*0, $k = 2n + 1$ for **9**), statistical analyses of intensity distributions, and the successful solution and refinement of the structures, the space groups were determined to be $P2_1/c$ (No. 14) for **1**, **3**, **4**, and **5**, *Pbca* (No. 61) for **6**, $P2_1/a$ (No. 14) for **7**, $P2_1$ (No. 4) for **9**, and $P\bar{1}$ (No. 2) for **2**.

The data were collected at a temperature of 23 ± 1 °C using the $\omega-2\theta$ scan technique to a maximum 2θ value of 50.0°. The ω scans of several intense reflections, made prior to data collection, had an average width at half-height of 0.29° for **1**, 0.15° for **2**, 0.31° for **3**, 0.16° for **4**, 0.40° for **5**, 0.28° for **6**, 0.15° for **7**, and 0.19° for **9**, with a takeoff angle of 6.0°. Scans of $(1.52 + 0.30 \tan \theta)°$ for **1**, $(1.31 + 0.30 \tan \theta)°$ for **2**, $(1.63 + 0.30 \tan \theta)°$ for **3**, $(1.73 + 0.30 \tan \theta)°$ for **4**, $(1.68 + 0.30 \tan \theta)°$ for **5**, $(1.37 + 0.30 \tan \theta)°$ for **6**, $(1.21 + 0.30 \tan \theta)°$ for **7**, and $(1.52 + 0.30 \tan \theta)°$ for **9** were made at speeds of 8.0°/min (in ω) for **1**, **3**, **5**, and **7**, 16.0°/min (in ω) for **2** and **6**, and 32.0°/min for **4** and **9**. The weak reflections ($I < 10.0\sigma(I)$) were rescanned (maximum of four rescans), and the counts were accumulated to assure good counting statistics. Stationary background counts were recorded on each side of the reflection. The ratio of peak counting time to background counting time was 2:1. The diameter of the incident beam collimator was 1.0 mm, and the crystal to detector distance was 285 mm.

(18) Paul, R. C.; Bhasin, K. K.; Chadha, R. K. *J. Inorg. Nucl. Chem.* **1975**, *37*, 2337.
(19) McCormick, B. J.; Stormer, B. P. *Inorg. Chem.* **1972**, *11*, 729.

Table 1. Crystallographic Data for $Me_2Te[S_2CN(CH_2)_3CH_2]_2$ **(1)**, $Me_2Te[S_2CN(CH_2)_4CH_2]_2$ **(2)**, $Me_2Te\{[S_2CN(CH_2)_3CH_2][S_2CN(CH_2)_4CH_2]\}$ **(3)**, $Me_2TeCl[S_2CN(CH_2)_3CH_2]$ **(4)**, $Me_2TeBr[S_2CN(CH_2)_3CH_2]$ **(5)**, $Me_2TeI[S_2CN(CH_2)_3CH_2]$ **(6)**, $Me_2TeCl[S_2CN(CH_2)_4CH_2]_2$ **(7)**, and Me

	1	**2**	**3**	**4**	**5**	**6**	**7**	**9**
chem formula	$C_{12}H_{22}N_2S_4Te$	$C_{14}H_{26}N_2S_4Te$	$C_{13}H_{24}N_2S_4Te$	$C_7H_{14}NS_2ClTe$	$C_7H_{14}NS_2BrTe$	$C_7H_{14}NS_2ITe$	$C_8H_{16}NS_2ClTe$	$C_8H_{16}NS_2ITe$
fw, g mol^{-1}	450.16	478.21	464.19	339.37	383.82	430.82	353.39	444.85
a, Å	6.38(1)	9.624(3)	6.55(1)	9.951(3)	10.085(4)	13.951(6)	9.756(2)	6.019(3)
b, Å	18.902(7)	12.904(3)	19.716(6)	6.386(3)	6.446(4)	19.849(8)	11.242(2)	8.986(4)
c, Å	14.672(6)	9.008(2)	14.990(9)	18.834(3)	19.020(5)	9.261(4)	12.028(3)	13.012(2)
α, deg		98.29(2)						
β, deg	97.73(6)	111.19(2)	95.27(8)	95.32(2)	95.08(3)		92.26(3)	100.61(3)
γ, deg		99.64(2)						
V, Å^3	1752(2)	1002.5(4)	1928(3)	1191.7(6)	1231.7(8)	2564(1)	1318.2(7)	691.7(6)
space group	$P2_1/c$ (No. 14)	$P\bar{1}$ (No. 2)	$P2_1/c$ (No. 14)	$P2_1/c$ (No. 14)	$P2_1/c$ (No. 14)	*Pbca* (No. 61)	$P2_1/a$ (No. 14)	$P2_1$ (No. 4)
Z	4	2	4	4	4	8	4	2
ρ_{calcd}, g cm^{-3}	1.71	1.58	1.60	1.89	2.07	2.23	1.78	2.14
T, °C	23	23	23	23	23	23	23	23
μ, cm^{-1}	21.64	18.83	19.55	30.20	59.17	50.12	27.34	46.20
R^a	0.0636	0.0504	0.0618	0.0358	0.0559	0.0392	0.0438	0.0364
$R_w{}^b$	0.0642	0.0454	0.0511	0.0314	0.0469	0.0326	0.0442	0.0305

[a] $R = \sum||F_o| - |F_c||/\sum|F_o|$. [b] $R_w = [\sum w(|F_o| - |F_c|)^2/\sum wF_o^2)]^{1/2}$.

Of the 3501 (for **1**), 3779 (for **2**), 3831 (for **3**), 2450 (for **4**), 2530 (for **5**), 2582 (for **6**), 2614 (for **7**), and 1438 (for **9**) reflections which were collected, 3211 (for **1**), 3549 (for **2**), 3508 (for **3**), 2311 (for **4**), 2387 (for **5**), 2462 (for **7**), and 1307 (for **9**) were unique (R_{int} = 0.211, 0.066, 0.249, 0.136, 0.126, 0.249, 0.147, and 0.076 for **1**, **2**, **3**, **4**, **5**, **6**, **7**, and **9**, respectively). The intensities of three representative reflections that were measured after every 150 reflections remained constant throughout data collection, indicating crystal and electronic stability, except in the case of **4** where the standards decreased by 12.7%. A decay correction was applied to **4**.

The linear absorption coefficient for Mo Kα is 21.64 cm^{-1} (for **1**), 18.83 cm^{-1} (for **2**), 19.55 cm^{-1} (for **3**), 30.20 cm^{-1} (for **4**), 59.17 cm^{-1} (for **5**), 50.12 cm^{-1} (for **6**), 27.34 cm^{-1} (for **7**), and 46.20 cm^{-1} (for **9**). An empirical absorption correction, based on the program DIFABS,[20] was applied which resulted in transmission factors ranging from 0.78 to 1.11 (for **1**), 0.79 to 1.14 (for **2**), 0.53 to 1.25 (for **3**), 0.84 to 1.12 (for **4**), 0.76 to 1.09 (for **5**), 0.82 to 1.08 (for **6**), 0.84 to 1.10 (for **7**), and 0.80 to 1.17 (for **9**). The data were corrected for Lorentz and polarization effects.

The structures were solved by direct methods.[21] In general, as many of the non-hydrogen atoms were refined anisotropically as was reasonable on the basis of the amount of $I > 3.00\sigma(I)$ data available. Thus, only the tellurium and sulfur atoms were refined anisotropically for **1** and **7**, the nitrogen atoms were also included for **3** and **5**, all non-hydrogen atoms except the carbon atoms of the rings were refined anisotropically for **2** and **9**, and all non-hydrogen atoms were refined anisotropically for **4** and **6**. Hydrogen atoms attached to carbon were included in their idealized positions with C−H set at 0.95 Å and with isotropic thermal parameters set at 1.2 times that of the carbon atom to which they were attached. The final cycle of full-matrix least-squares refinement[22] was based on 825 (for **1**), 1545 (for **2**), 884 (for **3**), 1196 (for **4**), 787 (for **5**), 1107 (for **6**), 725 (for **7**), and 827 (for **9**) observed reflections ($I > 3.00\sigma(I)$) and 102 (for **1**), 140 (for **2**), 106 (for **3**), 109 (for **4**), 74 (for **5**), 109 (for **6**), 73 (for **7**), and 92 (for **9**) variable parameters and converged (largest parameter shift was 0.001 times its esd in all cases) with unweighted and weighted agreement factors of $R = \sum||F_o| - |F_c||/\sum|F_o| = 0.0636$ (for **1**), 0.0504 (for **2**), 0.0618 (for **3**), 0.0358 (for **4**), 0.0559 (for **5**), 0.0392 (for **6**), 0.0438 (for **7**), and 0.0364 (for **9**) and $R_w = [\sum w(|F_o| - |F_c|)^2/\sum wF_o^2)]^{1/2} = 0.0642$ (for **1**), 0.0454 (for **2**), 0.0511 (for **3**), 0.0314 (for **4**), 0.0469 (for **5**), 0.0326 (for **6**), 0.0442 (for **7**), and 0.0305 (for **9**).

The standard deviations of an observation of unit weight[23] were 1.84 (for **1**), 1.49 (for **2**), 1.93 (for **3**), 1.32 (for **4**), 1.74 (for **5**), 1.44 (for **6**), 1.14 (for **7**), and 1.19 (for **9**). The weighting scheme was based on counting statistics and included a factor (p = 0.001 for **1**, 0.002 for **9**, 0.004 for **6**, 0.005 for **2**, **3**, **4**, and **5**, and 0.018 for **7**) to downweight the intense reflections. Plots of $\sum w(|F_o| - |F_c|)^2$ versus $|F_o|$, reflection order in data collection, sin θ/λ, and various classes of indices showed no unusual trends. The maximum and minimum peaks on the final difference Fourier map corresponded to 0.76 and −0.84 e/Å^3 for **1**, 1.15 and −0.60 e/Å^3 for **2**, 0.53 and −0.52 e/Å^3 for **3**, 0.47 and −0.52 e/Å^3 for **4**, 0.80 and −0.73 e/Å^3 for **5**, 0.84 and −0.74 e/Å^3 for **6**, 0.54 and −0.53 e/Å^3 for **7**, and 0.65 and −0.76 e/Å^3 for **9**, respectively.

Neutral-atom scattering factors were taken from Cromer and Waber.[24] Anomalous dispersion effects were included in F_c;[25] the values for $\Delta f'$ and $\Delta f''$ were those of Cromer.[26] All calculations were performed using the TEXSAN[27] crystallographic software package of the Molecular Structure Corp.

The final atomic coordinates and equivalent isotropic thermal parameters for the non-hydrogen atoms are given in Tables 2−9, important distances and bond angles in Tables 10−17, and ORTEP diagrams in Figures 1−10. Additional crystallographic data are available as Supporting Information.

Calculation of Pauling Bond Order. We have introduced an adjustment to Pauling's calculation of partial bond orders,[28] which was essentially based on the C−C single bond, to readily obtain estimates of the partial bond orders within these tellurium complexes.[2] Thus, Pauling's relationship is modified so that for $n = 10^X$, $X = [1.54(d - d_n)/d]/0.6$ or $X = 2.57(d - d_n)/d$, where d_n is the bond length for bond number, n, and d is the length of the single bond of the same type. On the basis of the assumption that in these compounds the appropriate Te−S single bond length is the average in **1**, **2**, and **3**, of 2.62 Å, typical calculated values of the lengths of Te···S partial bonds for various values of n are as follows: 2.62 Å (n = 1.0), 2.75 (0.75), 2.93 (0.50), 3.24 (0.25), and 3.64 (0.10). Similarly, on the basis of the assumption that the appropriate Te−Cl, Te−Br, and Te−I single bond lengths are those found in the corresponding Me_2TeX_2 compounds of 2.51, 2.68,

(20) Walker, N; Stuart, D. *Acta Crystallogr*. **1983**, *A39*, 153.
(21) Sheldrick, G. M. *Crystallographic Computing 3*; Sheldrick, G. M., Kruger, C., Goddard, R., Eds.; Oxford University Press: England, 1985; p 175.
(22) Least-squares function minimized: $\sum w(|F_o| - |F_c|)^2$, where $w = 4F_o^2/(F_o^2)$, $\sigma^2(F_o^2) = [S^2(C + R^2B) + (pF_o^2)^2]/(Lp)^2$, S = scan rate, C = total integrated peak count, R = ratio of scan time to background counting time, Lp = Lorentz-polarization factor, and p = p factor.
(23) Standard deviation of an observation of unit weight: $[\sum w(|F_o| - |F_c|)^2/N_o - N_v)^{1/2}$, where N_o= number of observations and N_v = number of variables.
(24) Cromer, D. T.; Waber, J. T. *International Tables for X-ray Crystallography*; Kynoch Press: Birmingham, England, 1974; Vol. IV, Table 2.2 A.
(25) Ibers, J. A.; Hamilton, W. C. *Acta Crystallogr*. **1964**, *17*, 781.
(26) Cromer, D. T. *International Tables for X-ray Crystallography*; Kynoch Press: Birmingham, England, 1974; Vol. IV, Table 2.3.1.
(27) *TEXSAN-TEXRAY Structure Analysis Package*; Molecular Structure Corp.: Woodlands, TX, 1985.
(28) Pauling, L. *J. Am. Chem. Soc*. **1947**, *69*, 542, and *The Nature of the Chemical Bond*, 3rd ed.; Cornell University Press: Ithaca, NY, 1960; p 255.

Table 2. Final Fractional Coordinates and *B*(eq) for Non-Hydrogen Atoms of $Me_2Te[S_2CN(CH_2)_3CH_2]_2$ **(1)** with Standard Deviations in Parentheses

atom	*x*	*y*	*z*	*B*(eq), Å^2
Te(1)	0.4231(3)	0.3909(1)	0.6578(2)	2.81(8)
S(1)	0.252(1)	0.4364(5)	0.7984(6)	4.3(5)
S(2)	0.645(1)	0.3533(5)	0.8588(7)	4.8(5)
S(3)	0.530(1)	0.3778(5)	0.4903(6)	4.0(4)
S(4)	0.852(1)	0.3002(5)	0.6207(6)	4.3(5)
N(1)	0.375(3)	0.395(2)	0.969(2)	3.3(5)
N(2)	0.867(3)	0.315(1)	0.442(2)	2.5(5)
C(1)	0.182(4)	0.454(2)	0.580(2)	3.7(7)
C(2)	0.658(4)	0.473(2)	0.681(2)	3.4(7)
C(3)	0.425(4)	0.396(2)	0.883(2)	2.9(6)
C(4)	0.497(5)	0.362(2)	1.046(2)	4.7(9)
C(5)	0.387(7)	0.379(3)	1.125(3)	10(1)
C(6)	0.208(5)	0.419(2)	1.095(3)	5.3(9)
C(7)	0.186(5)	0.439(2)	0.991(2)	4.9(8)
C(8)	0.761(4)	0.326(2)	0.512(2)	2.9(6)
C(9)	0.797(5)	0.340(2)	0.344(2)	4.6(8)
C(10)	0.995(5)	0.330(2)	0.302(2)	4.1(8)
C(11)	1.099(5)	0.264(2)	0.356(2)	4.4(8)
C(12)	1.046(4)	0.269(1)	0.446(2)	2.7(7)

and 2.92 Å, respectively, for X = Cl, Br, and I; typical calculated values of the lengths of Te···X partial bonds for various values of *n* are as follows: for Te···Cl, 2.51 Å ($n = 1.0$), 2.63 (0.75), 2.80 (0.50), 3.10 (0.25), and 3.49 (0.10); for Te···Br, 2.68 Å ($n = 1.0$), 2.81 (0.75), 2.99 (0.50), 3.31 (0.25), and 3.71 (0.10); and for Te···I, 2.92 Å ($n = 1.0$), 3.06 (0.75), 3.26 (0.50), 3.60 (0.25), and 4.06 (0.10). The corresponding "valences" for partial bonds, which were calculated for the Te−I bonds in TeI_4, gave 3.16 Å ($n = 0.40$) and 3.50 (0.20),[29] which are compatible with our calculations.

Results and Discussion

The preparations of the pyrrolidyl and piperidyl dithioformate bis derivatives of dimethyltellurium(IV), $Me_2Te[S_2CN(CH_2)_3CH_2]_2$ **(1)** and $Me_2Te[S_2CN(CH_2)_4CH_2]_2$ **(2)**, are readily achieved in over 85% yield by the reaction of an excess of the sodium salt of the appropriate dithiocarbamate with dimethyltellurium dichloride in dichloromethane or toluene in accord with the equation

$$Me_2TeCl_2 + 2NaS_2CNR_2 \rightarrow Me_2Te[S_2CNR_2]_2 + 2NaCl$$

$$\{NR_2 = N(CH_2)_3CH_2,\ N(CH_2)_4CH_2\}$$

Dimethylhalo(pyrrolidyl and piperidyl dithioformato)tellurium(IV) compounds **(4**−**9)** can be similarly prepared in 83−89% yields by the reaction of equimolar amounts of the appropriate salt and dimethyltellurium dihalide

$$Me_2TeX_2 + NaS_2CNR_2 \rightarrow Me_2TeX[S_2CNR_2] + NaX$$

$$\{X = Cl,\ Br,\ or\ I;\ NR_2 = N(CH_2)_3CH_2,\ N(CH_2)_4CH_2\}$$

The mixed ligand species, $Me_2Te\{[S_2CN(CH_2)_3CH_2][S_2CN(CH_2)_4CH_2]\}$ **(3)**, can be formed in 87% yield by the addition of an equimolar amount of $NaS_2CN(CH_2)_4CH_2$ to $Me_2TeCl[S_2CN(CH_2)_3CH_2]$ formed *in situ*. All of these compounds are soluble in common organic solvents such as C_6H_6, $CHCl_3$, and CH_2Cl_2 and are formed as crystalline solids. The bis-substituted compounds, **1** and **2**, as well as **3** are obtained as X-ray quality crystals on recrystallization from mixed CH_2Cl_2/*n*-hexane or toluene/*n*-hexane solvents, as are five of the partially substituted derivatives, **4**, **5**, **6**, **7**, and **9**. These derivatives can be handled in the open air rather than under nitrogen and can be stored in closed vials without prior evacuation. In general the halo derivatives decompose on heating above 100 °C, whereas the fully substituted species have sharp melting points. Although all compounds appeared to be stable at room temperature, they were stored in the refrigerator as a precaution.

Molecular Structures of $Me_2Te[S_2CN(CH_2)_3CH_2]_2$ (1), $Me_2Te[S_2CN(CH_2)_4CH_2]_2$ (2), $Me_2Te\{[S_2CN(CH_2)_3CH_2]$-

(29) Brown, I. D. *Acta Crystallogr.* **1977**, *B33*, 1305.

Table 3. Final Fractional Coordinates and *B*(eq) for Non-Hydrogen Atoms of $Me_2Te[S_2N(CH_2)_4CH_2]_2$ **(2)** with Standard Deviations in Parentheses

atom	*x*	*y*	*z*	*B*(eq), Å^2
Te(1)	0.0505(1)	0.73888(8)	0.4602(1)	3.41(3)
S(1)	0.2445(4)	0.9157(3)	0.6636(5)	4.8(2)
S(2)	0.3730(5)	0.7218(3)	0.7067(5)	5.3(2)
S(3)	−0.1618(4)	0.5684(3)	0.2781(5)	4.3(2)
S(4)	−0.0607(5)	0.7016(3)	0.0741(5)	5.1(2)
N(1)	0.540(1)	0.922(1)	0.822(1)	5.1(5)
N(2)	−0.232(2)	0.506(1)	−0.033(2)	11.4(8)
C(1)	−0.111(2)	0.838(1)	0.405(2)	4.4(6)
C(2)	−0.012(2)	0.691(1)	0.646(2)	5.7(7)
C(3)	0.399(2)	0.855(1)	0.737(2)	4.3(6)
C(4)	0.676(2)	0.884(1)	0.895(2)	5.2(3)
C(5)	0.778(2)	0.904(1)	0.801(2)	5.7(4)
C(6)	0.815(2)	1.022(1)	0.801(2)	7.1(4)
C(7)	0.674(2)	1.066(1)	0.740(2)	6.1(4)
C(8)	0.576(2)	1.041(1)	0.834(2)	5.7(4)
C(9)	−0.157(2)	0.589(1)	0.093(2)	4.7(6)
C(10)	−0.223(3)	0.500(2)	−0.202(3)	10.7(6)
C(11)	−0.368(2)	0.469(2)	−0.317(2)	10.0(6)
C(12)	−0.452(2)	0.356(2)	−0.320(2)	8.2(5)
C(13)	−0.444(2)	0.352(2)	−0.146(3)	9.1(5)
C(14)	−0.294(2)	0.389(2)	−0.026(3)	10.1(6)

Table 4. Final Fractional Coordinates and *B*(eq) for Non-Hydrogen Atoms of $Me_2Te\{[S_2CN(CH_2)_3CH_2][S_2CN(CH_2)_4CH_2]\}$ **(3)** with Standard Deviations in Parentheses

atom	*x*	*y*	*z*	*B*(eq), Å^2
Te(1)	0.0850(3)	0.4557(1)	0.1454(1)	4.40(8)
S(1)	0.098(1)	0.3928(4)	−0.0090(5)	5.4(4)
S(2)	−0.261(1)	0.3482(4)	0.0861(5)	6.5(5)
S(3)	0.164(1)	0.5253(4)	0.2926(5)	6.1(5)
S(4)	−0.216(1)	0.4461(4)	0.3075(5)	6.6(5)
N(1)	−0.194(4)	0.316(1)	−0.076(2)	7.7(7)
N(2)	−0.111(3)	0.551(1)	0.404(1)	6.1(6)
C(1)	0.371(4)	0.499(1)	0.113(2)	6.4(7)
C(2)	0.229(4)	0.371(1)	0.212(2)	5.9(7)
C(3)	−0.132(5)	0.350(1)	−0.002(2)	6.2(7)
C(4)	−0.076(6)	0.305(2)	−0.158(3)	10(1)
C(5)	−0.235(8)	0.271(2)	−0.231(3)	16(1)
C(6)	−0.429(8)	0.261(2)	−0.191(3)	18(1)
C(7)	−0.393(6)	0.274(2)	−0.086(2)	10(1)
C(8)	−0.060(4)	0.509(1)	0.335(2)	4.1(6)
C(9)	−0.287(5)	0.544(2)	0.453(2)	8.0(8)
C(10)	−0.384(6)	0.609(2)	0.456(2)	11(1)
C(11)	−0.254(8)	0.663(2)	0.484(3)	16(1)
C(12)	−0.088(9)	0.670(3)	0.427(3)	19(2)
C(13)	0.030(5)	0.610(2)	0.434(2)	9(1)

Table 5. Final Fractional Coordinates and *B*(eq) for Non-Hydrogen Atoms of $Me_2TeCl[S_2CN(CH_2)_3CH_2]$ **(4)** with Standard Deviations in Parentheses

atom	*x*	*y*	*z*	*B*(eq), Å^2
Te(1)	0.28960(6)	0.2238(1)	0.75889(3)	2.70(2)
Cl(1)	0.0856(2)	0.3149(5)	0.6626(1)	4.7(1)
S(1)	0.4529(3)	0.0722(4)	0.8542(1)	3.4(1)
S(2)	0.4804(3)	0.5413(4)	0.8613(1)	3.6(1)
N(1)	0.6381(6)	0.268(1)	0.9336(3)	2.7(3)
C(1)	0.229(1)	−0.092(2)	0.7426(5)	4.0(5)
C(2)	0.149(1)	0.300(2)	0.8333(4)	4.5(5)
C(3)	0.5338(8)	0.302(1)	0.8879(4)	2.6(4)
C(4)	0.724(1)	0.435(2)	0.9674(6)	4.0(5)
C(5)	0.845(1)	0.319(3)	0.9996(9)	9(1)
C(6)	0.813(1)	0.106(3)	1.0066(8)	7.8(9)
C(7)	0.689(1)	0.061(2)	0.9573(6)	4.1(5)

Table 6. Final Fractional Coordinates and *B*(eq) for Non-Hydrogen Atoms of $Me_2TeBr[S_2CN(CH_2)_3CH_2]$ **(5)** with Standard Deviations in Parentheses

atom	*x*	*y*	*z*	*B*(eq), Å^2
Te(1)	0.2051(1)	0.2156(2)	0.23947(8)	3.22(7)
Br(1)	0.4165(2)	0.3098(5)	0.3411(1)	5.2(1)
S(1)	0.0411(6)	0.0692(9)	0.1447(4)	3.9(4)
S(2)	0.0235(6)	0.5351(9)	0.1418(4)	4.4(4)
N(1)	−0.134(1)	0.276(3)	0.0671(8)	3.6(9)
C(1)	0.256(2)	−0.105(4)	0.257(1)	6.9(7)
C(2)	0.345(2)	0.285(3)	0.169(1)	4.4(5)
C(3)	−0.031(2)	0.310(3)	0.114(1)	2.6(4)
C(4)	−0.187(3)	0.079(3)	0.043(2)	4.3(5)
C(5)	−0.308(3)	0.126(5)	−0.007(2)	9.2(9)
C(6)	−0.331(3)	0.340(6)	0.006(2)	8.7(8)
C(7)	−0.215(2)	0.450(4)	0.034(1)	4.6(6)

Table 7. Final Fractional Coordinates and *B*(eq) for Non-Hydrogen Atoms of $Me_2TeI[S_2CN(CH_2)_3CH_2]$ **(6)** with Standard Deviations in Parentheses

atom	*x*	*y*	*z*	*B*(eq), Å^2
I(1)	−0.05263(8)	0.28646(5)	0.0079(1)	4.42(5)
Te(1)	0.01057(6)	0.41857(4)	0.1358(1)	2.81(4)
S(1)	0.0612(3)	0.5240(2)	0.2684(4)	3.7(2)
S(2)	0.1873(3)	0.4975(2)	0.0103(6)	3.8(2)
N(1)	0.2140(8)	0.5935(5)	0.201(1)	2.8(6)
C(1)	−0.091(1)	0.4062(7)	0.305(2)	5(1)
C(2)	0.122(1)	0.3626(7)	0.238(2)	4.6(8)
C(3)	0.160(1)	0.5423(6)	0.161(1)	2.9(7)
C(4)	0.192(1)	0.6379(7)	0.326(2)	3.6(8)
C(5)	0.272(1)	0.6922(8)	0.316(2)	5(1)
C(6)	0.345(1)	0.6672(9)	0.223(2)	8(1)
C(7)	0.300(1)	0.6160(7)	0.123(2)	4.2(9)

Table 8. Final Fractional Coordinates and *B*(eq) for Non-Hydrogen Atoms of $Me_2TeCl[S_2CN(CH_2)_4CH_2]$ **(7)** with Standard Deviations in Parentheses

atom	*x*	*y*	*z*	*B*(eq), Å^2
Te(1)	0.1104(1)	0.1130(1)	0.1441(1)	3.40(5)
Cl(1)	0.0026(6)	0.1777(5)	−0.0545(4)	6.1(3)
S(1)	0.2441(5)	0.0481(5)	0.3139(4)	3.9(3)
S(2)	0.0168(5)	0.2111(5)	0.3764(4)	3.9(3)
N(1)	0.172(1)	0.080(1)	0.519(1)	3.9(3)
C(1)	0.273(2)	0.033(2)	0.056(2)	5.6(5)
C(2)	0.199(2)	0.283(2)	0.146(1)	4.5(4)
C(3)	0.141(2)	0.112(2)	0.415(1)	2.9(3)
C(4)	0.277(2)	−0.004(2)	0.554(1)	3.6(4)
C(5)	0.381(2)	0.059(2)	0.627(2)	5.3(5)
C(6)	0.321(2)	0.122(2)	0.724(2)	5.4(5)
C(7)	0.206(2)	0.198(2)	0.685(2)	4.8(5)
C(8)	0.100(2)	0.136(2)	0.614(1)	4.0(4)

Table 9. Final Fractional Coordinates and *B*(eq) for Non-Hydrogen Atoms of $Me_2TeI[S_2CN(CH_2)_4CH_2]$ **(9)** with Standard Deviations in Parentheses

atom	*x*	*y*	*z*	*B*(eq), Å^2
I(1)	1.1065(2)	0.4697	1.0962(1)	4.71(7)
Te(1)	1.0689(2)	0.3782(2)	0.86772(8)	2.89(4)
S(1)	1.0727(8)	0.3056(7)	0.6814(4)	4.1(2)
S(2)	0.6723(8)	0.4948(7)	0.6955(4)	4.2(2)
N(1)	0.720(2)	0.336(2)	0.529(1)	2.9(7)
C(1)	1.394(3)	0.271(2)	0.910(1)	5(1)
C(2)	1.213(3)	0.589(2)	0.850(1)	4(1)
C(3)	0.803(2)	0.374(3)	0.627(1)	3.6(7)
C(4)	0.851(3)	0.254(2)	0.463(1)	3.0(3)
C(5)	0.899(2)	0.361(2)	0.376(1)	3.3(3)
C(6)	0.674(3)	0.424(2)	0.313(1)	4.0(4)
C(7)	0.532(3)	0.494(2)	0.384(1)	3.2(4)
C(8)	0.503(2)	0.389(3)	0.471(1)	3.3(3)

Table 10. Important Distances (Å) and Interatomic Angles (deg) for $Me_2Te[S_2CN(CH_2)CH_2]_2$ **(1)**[a,b]

Te(1)−S(1)	2.606(9)	Te(1)−S(3)	2.647(8)
Te(1)−S(2)	3.18(1)	Te(1)−S(4)	3.33(1)
Te(1)−C(1)	2.15(3)	Te(1)−C(2)	2.15(3)
S(1)−C(3)	1.72(3)	S(2)−C(3)	1.70(3)
N(1)−C(3)	1.35(3)	N(1)−C(4)	1.43(3)
N(1)−C(7)	1.53(3)	C(4)−C(5)	1.46(5)
C(5)−C(6)	1.39(5)	C(6)−C(7)	1.56(4)
S(3)−C(8)	1.77(3)	S(4)−C(8)	1.69(3)
N(2)−C(8)	1.32(3)	N(2)−C(9)	1.52(4)
N(2)−C(12)	1.43(3)	C(9)−C(10)	1.49(4)
C(10)−C(11)	1.57(4)	C(11)−C(12)	1.41(4)
Te(1)···Te′(1)	6.38(1)		
S(1)···S(2)	2.99(1)	S(3)···S(4)	3.00(1)
S(1)−Te(1)−S(3)	162.2(3)	Te(1)−S(1)−C(3)	97.2(9)
S(1)−Te(1)−C(1)	83.8(8)	S(1)−C(3)−S(2)	122(2)
S(1)−Te(1)−C(2)	89.6(8)	S(1)−C(3)−N(1)	118(2)
S(3)−Te(1)−C(1)	79.2(8)	S(2)−C(3)−N(1)	119(2)
S(3)−Te(1)−C(2)	87.5(8)	N(1)−C(4)−C(5)	105(3)
C(1)−Te(1)−C(2)	97(1)	N(1)−C(7)−C(6)	96(3)
C(3)−N(1)−C(4)	126(3)	C(3)−N(1)−C(7)	118(3)
C(4)−N(1)−C(7)	116(2)	C(4)−C(5)−C(6)	109(4)
C(5)−C(6)−C(7)	114(3)	Te(1)−S(3)−C(8)	101(1)
S(3)−C(8)−S(4)	120(2)	S(3)−C(8)−N(2)	117(2)
S(4)−C(8)−N(2)	123(2)	N(2)−C(9)−C(10)	101(2)
N(2)−C(12)−C(11)	107(3)	C(8)−N(2)−C(9)	125(3)
C(8)−N(2)−C(12)	123(3)	C(9)−N(2)−C(12)	111(2)
C(9)−C(10)−C(11)	102(3)	C(10)−C(11)−C(12)	106(3)
S(1)−Te(1)−S(2)	61.3(3)	S(3)−Te(1)−S(4)	58.8(2)
S(1)−Te(1)−S(4)	137.7(2)	S(3)−Te(1)−S(2)	134.7(3)
S(2)···Te(1)−S(4)	76.4(2)	C(1)−Te(1)−S(2)	144.6(8)
C(1)−Te(1)−S(4)	137.9(8)	C(2)−Te(1)−S(2)	78.4(8)
C(2)−Te(1)−S(4)	80.1(8)		

[a] Symmetry equivalent position $(1 - x, y, z)$ is denoted by a prime. [b] Numbers in parentheses refer to esd's in the least significant digits.

$[S_2CN(CH_2)_4CH_2]$} (3), $Me_2TeCl[S_2CN(CH_2)_3CH_2]$ (4), $Me_2TeBr[S_2CN(CH_2)_3CH_2]$ (5), $Me_2TeI[S_2CN(CH_2)_3CH_2]$ (6), $Me_2TeCl[S_2CN(CH_2)_4CH_2]$ (7), and $Me_2TeI[S_2CN(CH_2)_4CH_2]$ (9). Dimethylbis(pyrrolidyl dithioformato)tellurium(IV) **(1)** and dimethyl(piperidyl dihioformato)(pyrrolidyl dithioformato)tellurium(IV) **(3)**, crystallize in the space group $P2_1/c$, whereas dimethylbis(piperidyl dithioformato)tellurium(IV) **(2)** crystallizes in the space group $P\bar{1}$. The ORTEP diagrams in Figures 1 and 3, part a, illustrate that in all three compounds the immediate environment about tellurium is the sawhorse structure typical of tellurium(IV) compounds, at least in the gas phase, in which the lone pair is assumed to be active stereochemically and occupying an equatorial position in a distorted trigonal bipyramid approximately at the location of the Te(1) label. The two methyl groups occupy the other two equatorial positions; the C−Te−C bond angle of 97(1), 93.3(5), and 94(1)° in **1**, **2**, and **3**, respectively, covering the range for those reported for the related *N*,*N*-dialkyl dithiocarbamate derivative, $Me_2Te[S_2CNMe_2]_2$ (93.9(2)°),[15] and the monothiocarbamate derivative, $Me_2Te[SCONEt_2]_2$ (96.6(3)°).[17]

The average value for the Te−C bond length of 2.14(2) Å is essentially the same as that in the $Me_2Te[S_2NCMe_2]_2$ analogue of 2.13(1) Å.[15] The axial positions are occupied by the sulfur atoms of the dithiocarbamate groups; the S−Te−S bond angle of 166.0(2)° in the mixed species, **3**, being close to the average value for the two bis compounds, **1** and **2**, 162.2(3) and 173.1(1)°, respectively. The average length of these axial Te−S bonds of 2.62(2) Å is similar to the values reported for related dithiocarbamate derivatives.[8,10,15] In all three molecules one of the Te−S bonds is longer than the other, but the average values are essentially the same in each compound. In general, when these two Te−S bond lengths differ, the sulfur atom of the longer bond has been found to be associated with the tellurium atom of an adjacent molecule, with a contact distance significantly less than the sum of the van der Waals radii of 3.86 Å. However, this is not the case in **1**−**3** because only in

Table 11. Important Distances (Å) and Interatomic Angles (deg) for $Me_2Te[S_2CN(CH_2)_4CH_2]_2$ **(2)**[a,b]

Te(1)−S(1)	2.635(4)	Te(1)−S(3)	2.595(4)
Te(1)−S(2)	3.162(4)	Te(1)−S(4)	3.183(4)
Te(1)−C(1)	2.14(1)	Te(1)−C(2)	2.11(1)
S(1)−C(3)	1.76(1)	S(2)−C(3)	1.66(1)
N(1)−C(3)	1.36(2)	N(1)−C(4)	1.44(2)
N(1)−C(8)	1.49(2)	C(4)−C(5)	1.52(2)
C(5)−C(6)	1.50(2)	C(6)−C(7)	1.51(2)
C(7)−C(8)	1.51(2)		
S(3)−C(9)	1.74(1)	S(4)−C(9)	1.66(1)
N(2)−C(9)	1.32(2)	N(2)−C(10)	1.55(2)
N(2)−C(14)	1.54(2)	C(10)−C(11)	1.35(2)
C(11)−C(12)	1.54(2)	C(12)−C(13)	1.55(4)
C(13)−C(14)	1.40(2)	Te(1)···Te′(1)	6.264(2)
S(1)···S(2)	2.985(5)	S(3)···S(4)	2.988(5)
S(1)−Te(1)−S(3)	173.1(1)	Te(1)−S(1)−C(3)	95.2(5)
S(1)−Te(1)−C(1)	85.1(4)	S(1)−C(3)−S(2)	121.8(9)
S(1)−Te(1)−C(2)	91.8(4)	S(1)−C(3)−N(1)	116(1)
S(3)−Te(1)−C(1)	91.0(4)	S(2)−C(3)−N(1)	122(1)
S(3)−Te(1)−C(2)	82.8(4)	N(1)−C(4)−C(5)	109(1)
C(1)−Te(1)−C(2)	93.3(5)	N(1)−C(8)−C(7)	108(1)
C(3)−N(1)−C(4)	123(1)	C(3)−N(1)−C(8)	125(1)
C(4)−N(1)−C(8)	112(1)	C(4)−C(5)−C(6)	110(1)
C(5)−C(6)−C(7)	113(1)	C(6)−C(7)−C(8)	111(1)
Te(1)−S(3)−C(9)	96.4(5)	S(3)−C(9)−S(4)	123.0(9)
S(3)−C(9)−N(2)	115(1)	S(4)−C(9)−N(2)	122(1)
N(2)−C(10)−C(11)	108(2)	N(2)−C(14)−C(13)	108(2)
C(9)−N(2)−C(10)	124(1)	C(9)−N(2)−C(14)	127(1)
C(10)−N(2)−C(14)	107(1)	C(12)−C(13)−C(14)	113(2)
C(10)−C(11)−C(12)	113(2)	C(11)−C(12)−C(13)	109(2)
S(1)−Te(1)−S(2)	61.2(1)	S(3)−Te(1)−S(4)	61.3(1)
S(1)−Te(1)−S(4)	123.1(1)	S(3)−Te(1)−S(2)	121.6(1)
S(2)···Te(1)−S(4)	126.1(1)	C(1)−Te(1)−S(2)	145.1(4)
C(1)−Te(1)−S(4)	78.5(4)	C(2)−Te(1)−S(2)	80.1(4)
C(2)−Te(1)−S(4)	142.7(4)		

[a] Symmetry equivalent position ($-x$, $1-y$, $1-z$) is denoted by a prime. [b] Numbers in parentheses refer to esd's in the least significant digits.

the mixed ligand species is there a Te···S internuclear distance less than 3.86 Å and then only marginally so.

In all three derivatives the apparently nonbonded sulfur atoms are oriented toward the tellurium center at Te−S distances ranging from 3.162(4) to 3.33(1) Å. These distances correspond to normalized Pauling partial bond orders of about 0.25, which is compatible with their being part of the coordination sphere and hence probably more correctly considered as part of unsymmetrical bidentate or anisobidentate ligands as demonstrated in Figures 2 and 3, part b. In $Me_2Te[S_2CN(CH_2)_3CH_2]_2$ **(1)**, the orientation of the two dithiocarbamates results in the five atoms S(1), S(2), S(3), S(4), and C(1) as well as Te(1), forming an approximate plane (mean deviation from plane of 0.097 Å) with C(2) above the plane (2.08(3) Å) to give a six-coordinate approximate pentagonal pyramidal arrangement about Te(1) or a pentagonal bipyramidal arrangement if the lone pair is assumed to be occupying the axial position *trans* to C(2) as is demonstrated by the projection used in Figure 2, part a. The two planar S_2CN cores of the dithiocarbamate groups have a dihedral angle of only 0.7(2)°. By contrast, in $Me_2Te[S_2CN(CH_2)_4CH_2]_2$ **(2)**, the orientation of the two dithiocarbamates results in a different arrangement about tellurium. The dihedral angle between the two planar S_2CN cores is now 69.6(2)°, and the four atoms S(1), S(2), S(3), and C(1) as well as Te(1) form an approximate plane (mean deviation from plane of 0.087 Å) with C(2) above the plane (1.96(2) Å) and S(4) below the plane (2.58(1) Å). Similarly, S(1), S(3), S(4), C(2), and Te(1) form an approximate plane (mean deviation from plane of 0.124 Å) with C(1) above the plane (2.05(2) Å) and S(2) below the plane (2.49(1) Å). Thus, the arrangement about tellurium is better

Table 12. Important Distances (Å) and Interatomic Angles (deg) for $Me_2Te[S_2CN(CH_2)_3CH_2][S_2CN(CH_2)_4CH_2]_2$ **(3)**[a,b]

Te(1)−S(1)	2.634(7)	Te(1)−S(3)	2.609(7)
Te(1)−S(2)	3.171(9)	Te(1)−S(4)	3.275(7)
Te(1)−C(1)	2.16(3)	Te(1)−C(2)	2.12(3)
S(1)−C(3)	1.74(3)	S(2)−C(3)	1.64(3)
N(1)−C(3)	1.33(3)	N(1)−C(4)	1.52(4)
N(1)−C(7)	1.53(4)	C(4)−C(5)	1.58(5)
C(5)−C(6)	1.47(6)	C(6)−C(7)	1.59(5)
S(3)−C(8)	1.69(2)	S(3)−C(8)	1.64(2)
N(2)−C(8)	1.39(2)	N(2)−C(9)	1.43(3)
N(2)−C(13)	1.52(3)	C(9)−C(10)	1.42(4)
C(10)−C(11)	1.41(5)	C(11)−C(12)	1.46(6)
C(12)−C(13)	1.42(5)		
S(1)···S(2)	2.99(1)	S(3)···S(4)	2.97(1)
Te(1)···S′(1)	3.754(8)	Te(1)···Te′(1)	4.732(4)
S(1)−Te(1)−S(3)	166.0(2)	Te(1)−S(1)−C(3)	95(1)
S(1)−Te(1)−C(1)	83.7(7)	S(1)−C(3)−S(2)	125(2)
S(1)−Te(1)−C(2)	89.5(7)	S(1)−C(3)−N(1)	114(2)
S(3)−Te(1)−C(1)	82.6(7)	S(2)−C(3)−N(1)	121(2)
S(3)−Te(1)−C(2)	88.4(7)	N(1)−C(4)−C(5)	105(3)
C(1)−Te(1)−C(2)	94(1)	N(1)−C(7)−C(6)	104(3)
C(3)−N(1)−C(4)	127(3)	C(3)−N(1)−C(7)	123(3)
C(4)−N(1)−C(7)	110(3)	C(4)−C(5)−C(6)	109(4)
C(5)−C(6)−C(7)	109(4)	Te(1)−S(3)−C(8)	96.0(9)
S(3)−C(8)−S(4)	127(2)	S(3)−C(8)−N(2)	116(2)
S(4)−C(8)−N(2)	117(2)	N(2)−C(9)−C(10)	109(3)
N(2)−C(13)−C(12)	108(4)	C(8)−N(2)−C(9)	126(2)
C(8)−N(2)−C(13)	120(2)	C(9)−N(2)−C(13)	114(2)
C(9)−C(10)−C(11)	115(4)	C(10)−C(11)−C(12)	111(5)
C(11)−C(12)−C(13)	108(4)	C(2)−Te(1)−S(4)	82.9(7)
S(1)−Te(1)−S(2)	61.3(2)	S(3)−Te(1)−S(4)	59.3(2)
S(1)−Te(1)−S(4)	134.0(2)	S(3)−Te(1)−S(2)	132.1(2)
S(2)−Te(1)−S(4)	72.8(2)	C(1)−Te(1)−S(2)	144.8(7)
C(1)−Te(1)−S(4)	141.8(7)	C(2)−Te(1)−S(2)	72.8(7)

[a] Symmetry equivalent position ($-x$, $1-y$, $-z$) is denoted by a prime. [b] Numbers in parentheses refer to esd's in the least significant digits.

Table 13. Important Distances (Å) and Interatomic Angles (deg) for $Me_2TeCl[S_2CN(CH_2)CH_2]$ **(4)**[a,b]

Te(1)−Cl(1)	2.658(2)	Te(1)−S(1)	2.501(3)
Te(1)−C(1)	2.12(1)	Te(1)−C(2)	2.124(8)
S(1)−C(3)	1.763(6)	S(2)−C(3)	1.681(9)
N(1)−C(3)	1.304(9)	N(1)−C(4)	1.48(1)
N(1)−C(7)	1.47(1)	C(4)−C(5)	1.49(2)
C(5)−C(6)	1.41(2)	C(6)−C(7)	1.50(2)
Te(1)−S(2)	3.281(3)	S(1)···S(2)	3.011(4)
Te(1)···S′(2)	3.562(3)	Te(1)···Te′(1)	5.3012(7)
Te(1)···Te″(1)	5.3012(7)		
Cl(1)−Te(1)−S(1)	168.05(9)	C(1)−Te(1)−C(2)	96.8(4)
Cl(1)−Te(1)−C(1)	85.5(3)	S(1)−Te(1)−C(1)	83.8(3)
Cl(1)−Te(1)−C(2)	83.9(2)	S(1)−Te(1)−C(2)	92.1(3)
Cl(1)−Te(1)−S(2)	129.03(8)	S(1)−Te(1)−S(2)	61.01(7)
S(2)−Te(1)−C(1)	144.5(3)	S(2)−Te(1)−C(2)	81.4(3)
Te(1)−S(1)−C(3)	100.5(3)	S(1)−C(3)−S(2)	121.9(5)
S(1)−C(3)−N(1)	114.1(7)	S(2)−C(3)−N(1)	124.0(8)
C(3)−N(1)−C(4)	124.0(9)	C(3)−N(1)−C(7)	125.6(9)
C(4)−N(1)−C(7)	110.4(7)	N(1)−C(4)−C(5)	103(1)
N(1)−C(7)−C(6)	104.8(6)	C(4)−C(5)−C(6)	109(1)
C(5)−C(6)−C(7)	108(1)		
Cl(1)−Te(1)···S′(2)	97.65(7)	S(1)−Te(1)···S′(2)	85.22(7)
C(1)−Te(1)···S′(2)	77.6(3)	C(2)−Te(1)···S′(2)	174.1(3)
S(2)−Te(1)···S′(2)	101.84(5)	Te(1)−S(2)···Te″(1)	101.49(7)

[a] Symmetry equivalent position ($1-x$, $y-{}^1/_2$, ${}^3/_2-z$) is denoted by a prime and ($1-x$, ${}^1/_2+y$, ${}^3/_2-z$) by a double prime. [b] Numbers in parentheses refer to esd's in the least significant digits.

described as a distorted octahedral, with the lone pair apparently inactive, as is illustrated by Figure 2, part b. In $Me_2Te\{[S_2CN(CH_2)_3CH_2][S_2CN(CH_2)_4CH_2]\}$ **(3)**, the orientation of the two dithiocarbamates is essentially the same as that in **1** so that S(1),S(2), S(3), S(4), C(1), and Te(1) form an approximate

Table 14. Important Distances (Å) and Interatomic Angles (deg) for $Me_2TeBr[S_2CN(CH_2)_3CH_2]$ **(5)**[a,b]

Te(1)−Br(1)	2.814(3)	Te(1)−S(1)	2.519(6)
Te(1)−C(1)	2.15(2)	Te(1)−C(2)	2.08(2)
S(1)−C(3)	1.79(2)	S(2)−C(3)	1.63(2)
N(1)−C(3)	1.32(2)	N(1)−C(4)	1.44(2)
N(1)−C(7)	1.49(2)	C(4)−C(5)	1.51(4)
C(5)−C(6)	1.42(3)	C(6)−C(7)	1.43(3)
Te(1)−S(2)	3.232(7)	S(1)···S(2)	3.009(8)
Te(1)···S′(2)	3.562(7)	Te(1)···Te′(1)	5.287(2)
Te(1)···Te″(1)	5.287(2)		
Br(1)−Te(1)−S(1)	169.0(2)	C(1)−Te(1)−C(2)	98.6(9)
Br(1)−Te(1)−C(1)	86.9(6)	S(1)−Te(1)−C(1)	83.2(4)
Br(1)−Te(1)−C(2)	83.1(5)	S(1)−Te(1)−C(2)	93.2(6)
Br(1)−Te(1)−S(2)	127.9(1)	S(1)−Te(1)···S(2)	61.6(2)
S(2)−Te(1)−C(1)	144.8(7)	S(2)···Te(1)−C(2)	82.6(6)
Te(1)−S(1)−C(3)	97.7(6)	S(1)−C(3)−S(2)	125(2)
S(1)−C(3)−N(1)	111(2)	S(2)−C(3)−N(1)	125(2)
C(3)−N(1)−C(4)	127(2)	C(3)−N(1)−C(7)	122(2)
C(4)−N(1)−C(7)	111(2)	N(1)−C(4)−C(5)	105(2)
N(1)−C(7)−C(6)	100(2)	C(4)−C(5)−C(6)	103(3)
C(5)−C(6)−C(7)	114(3)		
Br(1)−Te(1)···S′(2)	97.4(1)	S(1)−Te(1)···S′(2)	84.9(2)
C(1)−Te(1)···S′(2)	75.6(7)	C(2)−Te(1)···S′(2)	173.3(6)
S(2)−Te(1)···S′(2)	102.0(1)	Te(1)−S(2)···Te″(1)	102.1(2)

[a] Symmetry equivalent position ($-x$, $y - {}^1/_2$, ${}^1/_2 - z$) is denoted by a prime and ($-x$, ${}^1/_2 - y$, ${}^1/_2 - z$) by a double prime. [b] Numbers in parentheses refer to esd's in the least significant digits.

Table 15. Important Distances (Å) and Interatomic Angles (deg) for$Me_2TeI[S_2CN(CH_2)_3CH_2]$ **(6)**[a,b]

Te(1)−I(1)	3.009(1)	Te(1)−S(1)	2.527(4)
Te(1)−C(1)	2.13(1)	Te(1)−C(2)	2.13(1)
S(1)−C(3)	1.74(1)	S(2)−C(3)	1.70(1)
N(1)−C(3)	1.32(1)	N(1)−C(4)	1.48(2)
N(1)−C(7)	1.47(2)	C(4)−C(5)	1.55(2)
C(5)−C(6)	1.42(2)	C(6)−C(7)	1.51(2)
Te(1)···S(2)	3.143(4)	S(1)···S(2)	3.014(6)
Te(1)···S′(2)	3.497(5)	Te(1)···Te′(1)	4.106(2)
I(1)−Te(1)−S(1)	174.1(1)	C(1)−Te(1)−C(2)	95.4(6)
I(1)−Te(1)−C(1)	89.7(4)	S(1)−Te(1)−C(1)	85.6(4)
I(1)−Te(1)−C(2)	86.2(4)	S(1)−Te(1)−C(2)	90.7(4)
I(1)−Te(1)−S(2)	121.23(9)	S(1)−Te(1)−S(2)	63.1(1)
S(2)−Te(1)−C(1)	148.4(4)	S(2)−Te(1)−C(2)	81.7(4)
Te(1)−S(1)−C(3)	96.9(7)	S(1)−C(3)−S(2)	122.5(8)
S(1)−C(3)−N(1)	117(1)	S(2)−C(3)−N(1)	121((1)
C(3)−N(1)−C(4)	124((1)	C(3)−N(1)−C(7)	124((1)
C(4)−N(1)−C(7)	112(1)	N(1)−C(4)−C(5)	103(1)
N(1)−C(7)−C(6)	104(1)	C(4)−C(5)−C(6)	108(1)
C(5)−C(6)−C(7)	108(2)		
I(1)−Te(1)···S′(2)	91.83(8)	S(1)−Te(1)···S′(2)	90.8(1)
C(1)−Te(1)···S′(2)	79.4(4)	C(2)−Te(1)···S′(2)	174.4(4)
S(2)−Te(1)···S′(2)	103.81(9)	Te(1)−S(2)···Te′(1)	76.19(9)

[a] Symmetry equivalent position ($-x$, $1 - y$, $-z$) is denoted by a prime. [b] Numbers in parentheses refer to esd's in the least significant digits.

pentagonal plane (mean deviation from plane of 0.038 Å) with C(2) above the plane (2.06(3) Å). A different projection is provided in Figure 3, part b, to emphasize the pentagonal pyramidal arrangement of the core atoms in **3**. The difference between the distorted octahedral structure of **2** and those of **1** and **3** can also be considered in terms of a reorientation of the ligand that includes the Te(1)−S(3) bond. Relative to its position in **1** and **3**, this bond pivots to take the S(4) atom out of the pentagonal plane so that the value of the angle C(1)−Te(1)−S(4) becomes 78.5(4)° in **2** compared to 137.9(8) and 141.8(7)° in **1** and **3**, respectively, as can be seen in Figure 2 and Tables 12−14. The average Te−S−C angle for the three compounds is 97(2)°, the average bite angle is 60.5(12)°, and the average bite length is 2.99(1) Å; all of which are typical of the dialkyl dithiocarbamate ligands attached to tellurium.[8,10,15]

Table 16. Important Distances (Å) and Interatomic Angles (deg) for $Me_2TeCl[S_2CN(CH_2)_4CH_2]$ **(7)**[a,b]

Te(1)−Cl(1)	2.672(5)	Te(1)−S(1)	2.489(5)
Te(1)−C(1)	2.14(2)	Te(1)−C(2)	2.10(2)
S(1)−C(3)	1.77(2)	S(2)−C(3)	1.69(3)
N(1)−C(3)	1.32(2)	N(1)−C(4)	1.45(2)
N(1)−C(8)	1.50(2)	C(4)−C(5)	1.49(3)
C(5)−C(6)	1.50(2)	C(6)−C(7)	1.47(3)
C(7)−C(8)	1.49(2)	S(1)···S(2)	2.995(7)
Te(1)−S(2)	3.171(5)	Te(1)···Cl′(1)	3.601(6)
Te(1)···Te′(1)	4.745(2)		
Cl(1)−Te(1)−S(1)	171.2(2)	C(1)−Te(1)−C(2)	94.3(8)
Cl(1)−Te(1)−C(1)	86.8(6)	S(1)−Te(1)−C(1)	84.8(6)
Cl(1)−Te(1)−C(2)	84.9(5)	S(1)−Te(1)−C(2)	93.1(5)
Cl(1)−Te(1)···S(2)	125.2(2)	S(1)−Te(1)···S(2)	62.5(1)
S(2)···Te(1)−C(1)	145.9(6)	S(2)···Te(1)−C(2)	78.8(5)
Te(1)−S(1)−C(3)	98.8(5)	S(1)−C(3)−S(2)	119.7(9)
S(1)−C(3)−N(1)	115(1)	S(2)−C(3)−N(1)	125(1)
C(3)−N(1)−C(4)	126(2)	C(3)−N(1)−C(8)	113(1)
C(4)−N(1)−C(8)	113(1)	N(1)−C(4)−C(5)	108(2)
N(1)−C(8)−C(7)	108(2)	C(4)−C(5)−C(6)	114(2)
C(5)−C(6)−C(7)	110(2)	C(6)−C(7)−C(8)	114(2)
Cl(1)−Te(1)···Cl′(1)	82.8(2)	S(1)−Te(1)···Cl′(1)	97.1(1)
C(1)−Te(1)···Cl′(1)	72.2(6)	C(2)−Te(1)···Cl′(1)	162.2(5)
S(2)−Te(1)···Cl′(1)	118.9(1)	Te(1)−Cl(1)···Te′(1)	97.2(2)

[a] Symmetry equivalent position ($-x$, $-y$, $-z$) is denoted by a prime. [b] Numbers in parentheses refer to esd's in the least significant digits.

Table 17. Important Distances (Å) and Interatomic Angles (deg) for $Me_2TeI[S_2CN(CH_2)_4CH_2]$ **(9)**[a,b]

Te(1)−I(1)	3.052(2)	Te(1)−S(1)	2.514(5)
Te(1)−C(1)	2.16(2)	Te(1)−C(2)	2.11(2)
S(1)−C(3)	1.76(2)	S(2)−C(3)	1.69(2)
N(1)−C(3)	1.32(2)	N(1)−C(4)	1.47(2)
N(1)−C(8)	1.47(2)	C(4)−C(5)	1.55(2)
C(5)−C(6)	1.55(2)	C(6)−C(7)	1.50(2)
C(7)−C(8)	1.50(2)	S(1)···S(2)	2.982(7)
Te(1)−S(2)	3.139(5)	Te(1)···I′(1)	3.872(4)
Te(1)···Te′(1)	5.812(2)	Te(1)···Te″(1)	5.812(2)
I(1)−Te(1)−S(1)	175.3(1)	C(1)−Te(1)−C(2)	93.2(7)
I(1)−Te(1)−C(1)	88.4(5)	S(1)−Te(1)−C(1)	87.7(5)
I(1)−Te(1)−C(2)	84.6(5)	S(1)−Te(1)−C(2)	92.9(5)
I(1)−Te(1)−S(2)	121.1(1)	S(1)−Te(1)−S(2)	62.5(1)
S(2)−Te(1)−C(1)	149.8(5)	S(2)−Te(1)−C(2)	84.1(5)
Te(1)−S(1)−C(3)	97.3(6)	S(1)−C(3)−S(2)	120(1)
S(1)−C(3)−N(1)	117(1)	S(2)−C(3)−N(1)	123(1)
C(3)−N(1)−C(4)	123(1)	C(3)−N(1)−C(8)	124(1)
C(4)−N(1)−C(8)	112(1)	N(1)−C(4)−C(5)	108(1)
N(1)−C(8)−C(7)	112(1)	C(4)−C(5)−C(6)	110(1)
C(5)−C(6)−C(7)	112(1)	C(6)−C(7)−C(8)	111(2)
I(1)−Te(1)···I′(1)	96.33(4)	S(1)−Te(1)···I′(1)	85.5(1)
C(1)−Te(1)···I′(1)	78.5(5)	C(2)−Te(1)···I′(1)	171.6(5)
S(2)−Te(1)···I′(1)	102.4(1)	Te(1)−I(1)···Te″(1)	113.61(5)

[a] Symmetry equivalent position ($2 - x$, ${}^1/_2 + y$, $2 - z$) is denoted by a prime and ($2 - x$, $y - {}^1/_2$, $2 - z$) by a double prime. [b] Numbers in parentheses refer to esd's in the least significant digits.

Of the three dimethylhalo(pyrrolidyl dithioformato)tellurium(IV) compounds, $Me_2TeCl[S_2CN(CH_2)_3CH_2]$ **(4)** and $Me_2TeBr[S_2CN(CH_2)_3CH_2]$ **(5)** are isostructural and crystallize in the space group $P2_1/c$, while $Me_2TeI[S_2CN(CH_2)_3CH_2]$ **(6)** crystallizes in the space group $Pbca$. The two dimethylhalo(piperidyl dithioformato)tellurium(IV) derivatives $Me_2TeCl[S_2CN(CH_2)_4CH_2]$ **(7)** and $Me_2TeI[S_2CN(CH_2)_4CH_2]$ **(9)** crystallize in the space groups $P2_1/a$ and $P2_1$, respectively. The ORTEP diagrams, which are presented in Figure 4, for compounds **4**−**6**, and Figure 5, for **7** and **9**, illustrate that, as with the fully substituted species **1**, **2**, and **3**, the immediate environment about tellurium may again be considered to be the sawhorse structure with the halogen atoms occupying the position of one of the sulfur atoms in **1**, **2**, or **3** and the supposed lone pair

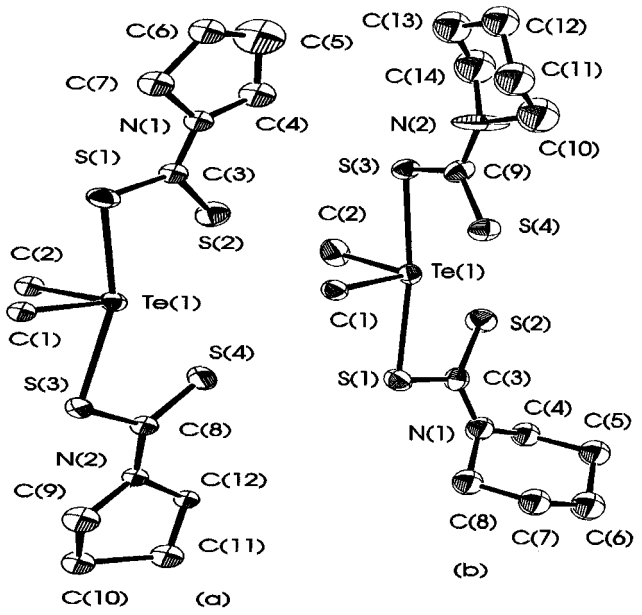

Figure 1. ORTEP plots of the molecules (a) $Me_2Te[S_2CN(CH_2)_3CH_2]_2$ **(1)** and (b) $Me_2Te[S_2CN(CH_2)_4CH_2]_2$ **(2)**. The atoms are drawn with 30% probability ellipsoids. Hydrogen atoms are omitted for clarity.

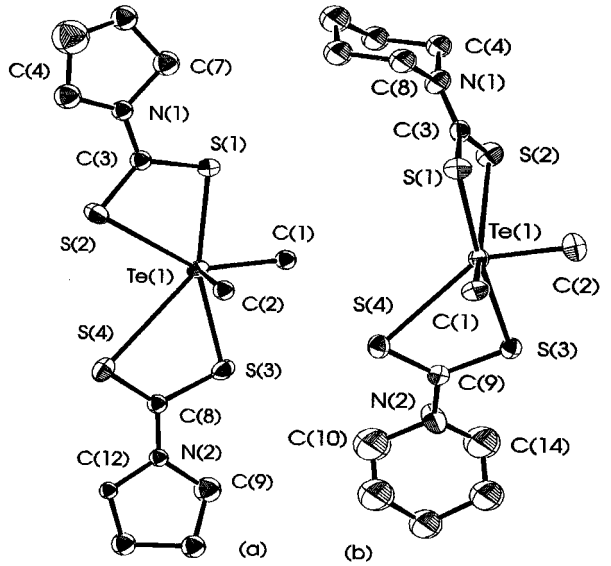

Figure 2. ORTEP plot of the molecules (a) $Me_2Te[S_2CN(CH_2)_3CH_2]_2$ **(1)** and (b) $Me_2Te[S_2CN(CH_2)_4CH_2]_2$ **(2)** showing the stereochemistry about tellurium when the intramolecular interactions leading to unsymmetrical bidentate ligands are included. The atoms are drawn with 30% probability ellipsoids. Hydrogen atoms are omitted for clarity.

approximately in the position of the Te(1) label. The average Te−C bond length of 2.12(3) Å in the five partially substituted derivatives (Tables 13−17) is essentially the same as in **1**−**3** and those found in the related monothiocarbamate monosubstituted compounds, $Me_2TeX[SCONEt_2]$ of 2.11(2) Å. However, the average Te−S distance in **4**, **5**, **6**, **7**, and **9** of 2.51(2) Å is considerably shorter (Tables 13−17) than those of the related Te−S bonds in **1**, **2**, and **3** (Tables 10−12) and corresponds to a bond order of 1.28. By contrast, the Te−X bonds are distinctly longer than in related R_2TeX_2 species, an average of 2.665(7) Å for **4** and **7** compared to 2.51(4) Å for α-Me_2TeCl_2,[30] 2.815(3) Å for Te−Br in **5** compared to 2.67(4) Å in Me_2TeBr_2,[31] and an average of 3.03(3) Å for Te−I in **6** and **9** compared to a range of 2.885(3)−2.994(3) Å in α-Me_2TeI_2.[32] On the basis of the bond order being 1.0 in R_2TeX_2, the bond orders for the Te−Cl, Te−Br, and Te−I bonds in these $Me_2TeX[S_2CN(CH_2)_nCH_2]$ species are 0.69, 0.72, and 0.80, respectively. The shortening of the Te−S bond and lengthening of the Te−X bonds appears to be an example of the *trans* influence operating on a main group metal.

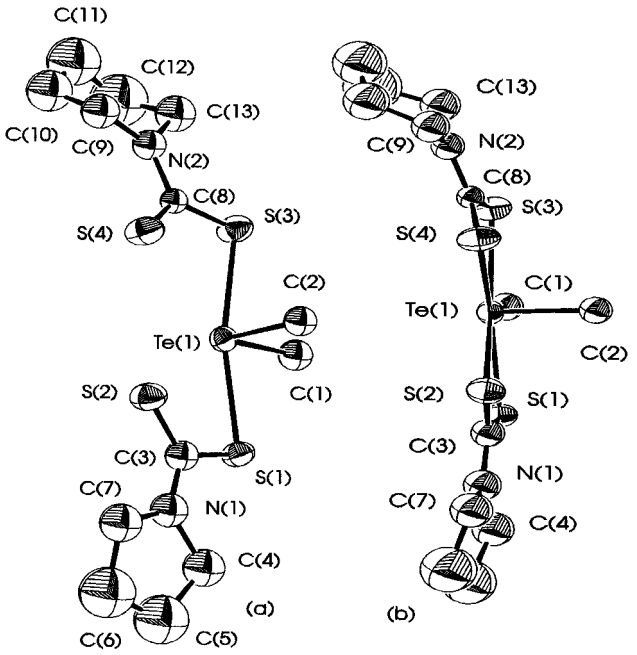

Figure 3. ORTEP plot of the molecule $Me_2Te\{[S_2CN(CH_2)_3CH_2][S_2CN(CH_2)_4CH_2]\}$ **(3)** showing the stereochemistry around tellurium (a) without and (b) with the inclusion of interactions. The atoms are drawn with 30% probability ellipsoids. Hydrogen atoms are omitted for clarity.

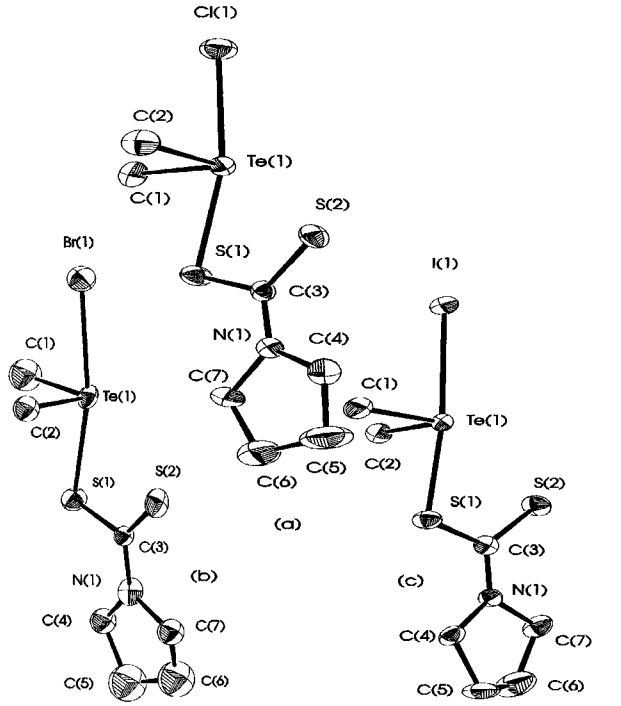

Figure 4. ORTEP plots of the molecules (a) $Me_2TeCl[S_2CN(CH_2)_3CH_2]$ **(4)**, (b) $Me_2TeBr[S_2CN(CH_2)_3CH_2]$ **(5)**, and (c) $Me_2TeI[S_2CN(CH_2)_3CH_2]$ **(6)**. The atoms are drawn with 30% probability ellipsoids. Hydrogen atoms are omitted for clarity.

(30) Christofferson, G. D.; Sparks, R. A.; McCullough, J. D. *Acta Crystallogr.* **1958**, *11*, 782.

(31) Drake, J. E.; Khasrou, L. N. Unpublished observations.

(32) Christofferson, G. D.; McCullough, J. D. *Acta Crystallogr.* **1958**, *11*, 249.

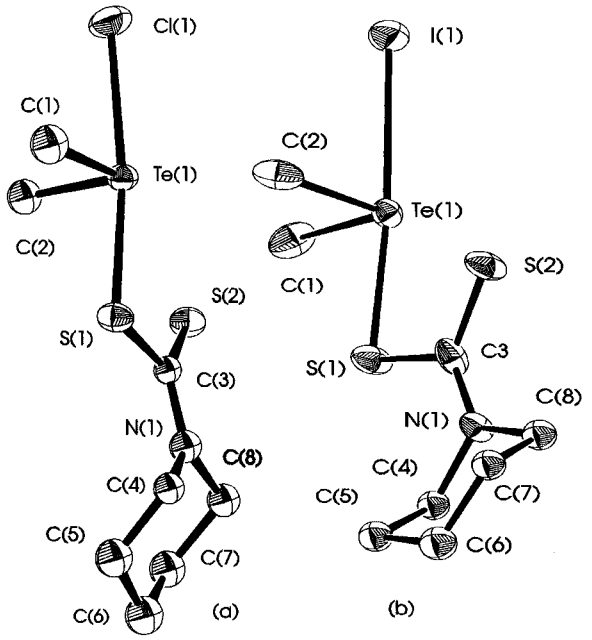

Figure 5. ORTEP plots of the molecules (a) $Me_2TeCl[S_2CN(CH_2)_4CH_2]$ **(7)** and (b) $Me_2TeI[S_2CN(CH_2)_4CH_2]$ **(9)**. The atoms are drawn with 30% probability ellipsoids. Hydrogen atoms are omitted for clarity.

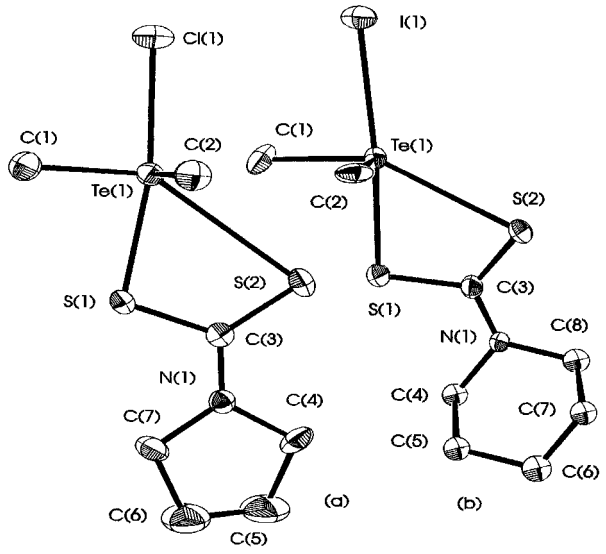

Figure 6. ORTEP plots of the molecules (a) $Me_2TeCl[S_2CN(CH_2)_3CH_2]$ **(4)** and (b) $Me_2TeI[S_2CN(CH_2)_4CH_2]$ **(9)** demonstrating the coplanarity of the sulfur atoms of the dithiocarbamate group with tellurium, chlorine, or iodine and one of the methyl carbon atoms. The atoms are drawn with 30% probability ellipsoids. Hydrogen atoms are omitted for clarity.

Further, as with the fully substituted derivatives, **1**−**3**, it is reasonable to consider each dithiocarbamate group as an unsymmetrical bidentate ligand by including the Te−S aniso bond in the coordination sphere. Despite the shorter Te(1)−S(1) bonds in **4**, **5**, **6**, **7**, and **9**, the aniso bonds, Te(1)−S(2), are of similar length to those in **1**−**3** covering the range 3.139(5)−3.281(3) Å, with bond orders again close to 0.25. The Te−S−C bond angle is essentially the same (average of 98(2)°) as in **1**−**3**, as are the bite angles, which range from 61.01(7) to 63.1(1)°, and the bite lengths (average of 3.00(1) Å). The orientation of the dithiocarbamate group is also similar in all five partially substituted species, so just two representative structural arrangements are given in Figure 6 for compounds **4** and **9**. The atoms S(1), S(2), X(1), C(1), and Te(1) form an approximate plane (mean deviation from plane of 0.064, 0.073, 0.065, 0.114, and 0.052 Å for **4**, **5**, **6**, **7**, and **9**, respectively) with C(2) above the plane (2.01(1), 2.02(2), 2.06(1), 2.01(2), and 2.04(2) Å for **4**, **5**, **6**, **7**, and **9**, respectively) to give a distorted square pyramidal arrangement about tellurium in all five cases or a distorted octahedral if the lone pair is now assumed to be occupying the position *trans* to C(2).

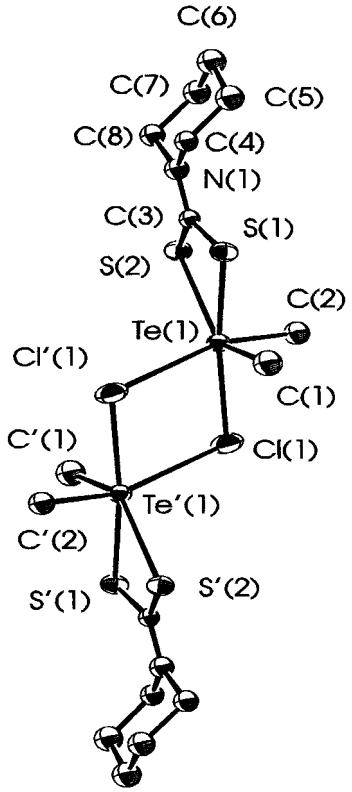

Figure 7. ORTEP plot of the molecule $Me_2TeCl[S_2CN(CH_2)_4CH_2]$ **(7)** showing intermolecular interactions involving the chlorine atoms leading to a dimer. The atoms are drawn with 30% probability ellipsoids. Hydrogen atoms are omitted for clarity.

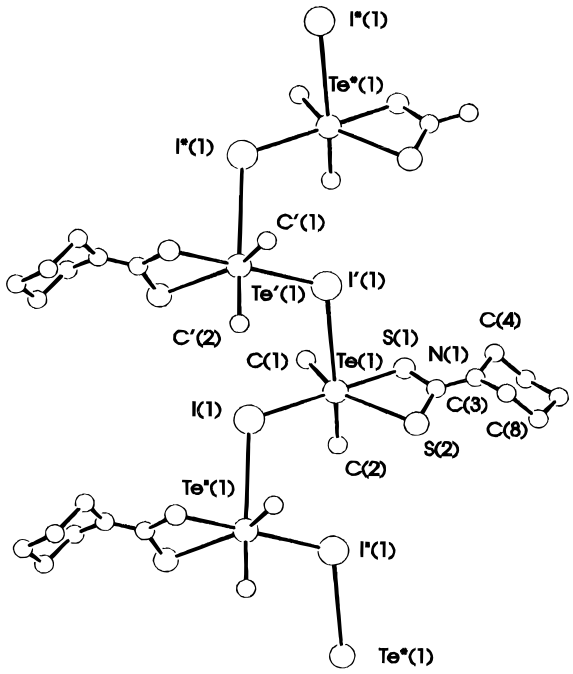

Figure 8. ORTEP plot using ideal spheres of the molecule $Me_2TeI[S_2CN(CH_2)_4CH_2]$ **(9)** showing intermolecular interactions involving the iodine atoms leading to a pseudopolymer. Hydrogen atoms are omitted for clarity.

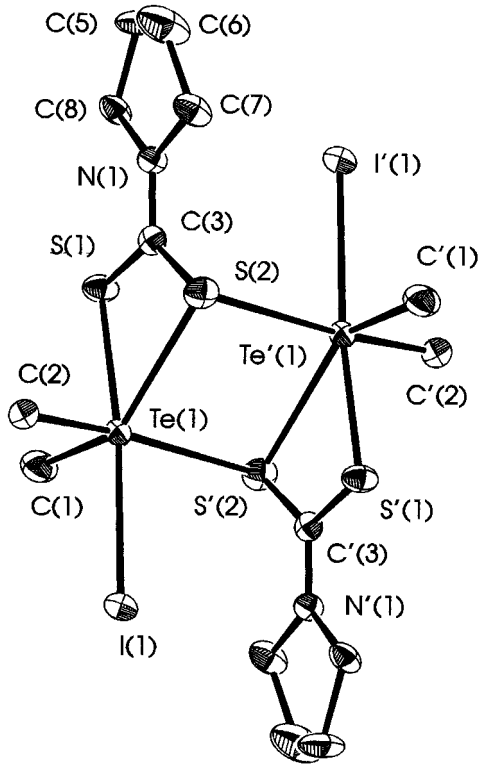

Figure 9. ORTEP plot of the molecule $Me_2TeI[S_2CN(CH_2)_3CH_2]$ **(4)** showing intermolecular interactions involving the aniso-bonded sulfur atoms leading to a dimer. The atoms are drawn with 30% probability ellipsoids. Hydrogen atoms are omitted for clarity.

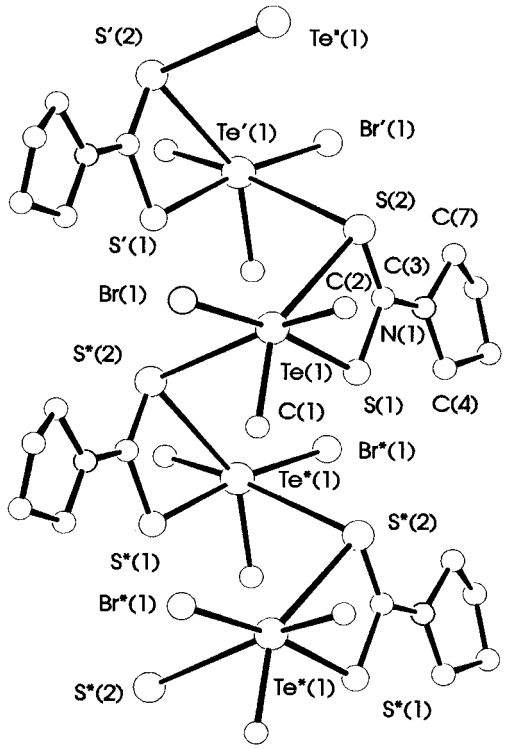

Figure 10. ORTEP plot using ideal spheres of the molecule $Me_2TeBr[S_2CN(CH_2)_3CH_2]$ **(5)** showing intermolecular interactions involving the aniso-bonded sulfur atoms leading to a pseudopolymer. Hydrogen atoms are omitted for clarity.

The phenomenon of significant change in the Te−X and Te−S bond lengths was also noted for the series of monothiocarbamates, $Me_2TeX[SCONEt_2]$, where the differences were slightly more marked, with the Te−S bonds even shorter (an average of 2.48(1) Å) and the Te−Br and Te−I bonds slightly longer at 2.905(1) and 3.116(1) Å, respectively.[17] In all three compounds $Me_2TeX[SCONEt_2]$, X = Cl, Br, and I, the halogen atoms have intermolecular associations with an adjacent tellurium atom to form an unsymmetrical Te−X···Te′ bridge. The Te···X′ intermolecular distances of 3.465(1), 3.547(2), and 3.704(1) Å, respectively, for Te···Cl′, Te···Br′, and Te···I′ correspond to bond orders of 0.10, 0.15, and 0.20, respectively. These are similar to those found in the Me_2TeX_2 species where the average Te···X′ distances are 3.50, 3.61, and 3.88 Å, respectively, for X = Cl, Br, and I.[30−32] Also, as with the dihalides, the X−Te···X′ and Te−X···Te′ angles are both very close to 90°, so the bridging systems essentially form a rectangle with *cis* Te−X and Te···X′ bonds within the dimeric species. Thus, it is surprising to find that there are no intermolecular interactions involving the halogen atoms in the pyrrolidyl derivatives, **4**−**6**. However, for the piperidyl derivatives, $Me_2TeCl[S_2CN(CH_2)_4CH_2]$ **(7)** and $Me_2TeI[S_2CN(CH_2)_4CH_2]$ **(9)**, there are Te···Cl′ and Te···I′ distances of 3.601(6) and 3.872(4) Å, respectively, corresponding to a bond order of only 0.08 for **7** but of 0.15 for **9**. The inclusion of this interaction in the coordination sphere, along with the stronger intramolecular Te−S interaction, leads to a distorted octahedral environment about tellurium in which the Te···X′ bond, rather than a lone pair, is *trans* to C(2); the C(2)−Te(1)···Cl′(1) and C(2)−Te(1)···I′(1) angles being 162.2(5) and 171.6(5)°, respectively (Tables 16 and 17). The Te···Cl′ linkage is more nebulous but apparently leads to the formation of dimeric units in **7** with Te−Cl(1)···Te′ and Cl−Te···Cl′ angles of 97.2(2) and 82.8(2)°, respectively (see Figure 8). By contrast, in **9**, rather than forming a dimeric association, the Te−I···Te links lead to an extended structure with the formation of a pseudopolymer (see Figure 7).

The absence of Te···X′ interactions in **4**−**6** is demonstrated by the fact that, in $Me_2TeI[S_2CN(CH_2)_3CH_2]$ **(6)**, the closest Te···I′ distance is over 5.0 Å. However, in all three molecules there are similar Te(1)···S(2)′ interactions of 3.562(3), 3.562(7), and 3.497(5) Å, respectively, for **4**, **5**, and **6** (Tables 13−15) which correspond to bond orders close to 0.15. In **6**, the S′(2) atom is apparently playing a role similar to those of the halogen atoms in the Me_2TeX_2 species in that dimeric units are formed by bridges in which the Te(1)−S(2)···Te′(1) and S(2)−Te(1)···S′(2) angles are 76.19(9) and 103.8(1)°, respectively (see Figure 9). The S′(2) atom is now *trans* to C(2) at 174.4(4)°, to again give a distorted octahedral environment about tellurium. By contrast, in $Me_2TeCl[S_2CN(CH_2)_3CH_2]$ **(4)** and $Me_2TeBr[S_2CN(CH_2)_3CH_2]$ **(5)**, which are isostructural, the Te(1)−S(2)···Te′ intermolecular interactions lead to an extended structure in the solid state in which pseudopolymers result from zigzag chains of S(2)−Te(1)−S′(2)−Te′(1)−S″(2) links (Figure 10). Once again, the immediate environment about tellurium is that of a distorted octahedral, with an apparently inactive lone pair, in which the weaker Te(1)−S′(2) bond is *trans* to Te(1)−C(2), with C(2)−Te(1)···S′(2) angles of 174.1(3) and 173.3(6)° for **4** and **5**, respectively. The shortening of the Te−S bond and lengthening of the Te−X bonds thus occurs regardless of whether the halogen atom is involved in intramolecular interactions, which confirms that the phenomenon is a result of the *trans* influence operating in these main group metal compounds rather than a result of inter- or intramolecular interactions.

As with related species, the dithiocarbamate groups are planar in all eight compounds with the three angles adding up to 360°. Despite variations from compound to compound, in general the (Te)S−C−N angles are all less than 120° at an average of 116(2)° for **1**, **2**, **3**, **4**, **5**, **6**, **7**, and **9**, whereas the average (Te)S−

Table 18. Selected IR[a] [Raman][b] Features and Their Assignments in the Vibrational Spectra of Me_2TeL_2 **(1)** and Me_2TeXL **(4−6)**, where L = $S_2CN(CH_2)_3(CH_2)$ and X = Cl, Br, and I, and of $Me_2TeL'_2$ **(2)**, Me_2TeLL' **(3)**, and Me_2TeXL' **(7−9)**, where L′ = $S_2CN(CH_2)_4CH_2$[c,d]

Me_2TeL_2 **(1)**	Me_2TeClL **(4)**	Me_2TeBrL **(5)**	Me_2TeIL **(6)**	assgnt
1432 s	1442 s	1444 s	1440 s	ν(C−NR_2)
[1428 (25)]	[1436 (5)]	[1442 (10)]	[1439 (15)]	
949 m	945 m	944 ms	942 m	ν(C═S)
[945 (15)]	[945 (5)]	[945 (5)]	[943 (5)]	
699 mw	690 sh	693 mw	697 mw	ν(C−STe)
[*e*]	[*e*]	[692 (5)]	[693 (5)]	
540 vw	540 sh	534 w	530 w, sh	ν(Te−C)$_{asym}$
[538 (50)]	[539 (100)]	[534 (80)]	[531 (50)]	
520 w	520 sh	515 w	520 w, sh	ν(Te−C)$_{sym}$
[519 (85)]	[521 (50)]	[519 (100)]	[520 (35)]	
315 s, br	354 m	352 s	339 s	ν(Te−S)[f]
[331 (100)]	[359 (40)]	[350 (65)]	[335 (100)]	
	208 s	137 m	108 m	ν(Te−X)[g]

$Me_2TeL'_2$ **(2)**	Me_2TeLL' **(3)**	Me_2TeClL' **(7)**	Me_2TeBrL' **(8)**	Me_2TeIL' **(9)**	assgnt
1468 s	1473 ms	1475 m	1481 s	1479 vs	ring
[1470 (60)]	[1472 (20)]	[1471 (20)]	[1480 (65)]	1481 (60)]	and
1421 s	1422 vs, br[h]	1432 s	1437 s	1433 s	ν(C−NR_2)
[1425 (20)]	[1425 (20)]	[1434 (20)]	[1433 (20)]	[1435 (15)]	
966 m	971 m	972 m	967 m	961 m	ν(C═S)
[967 (50)]	[973 (30)]	[971 (40)]	[966 (60)]	[967 (50)	
	947 ms				
	[946 (15)]				
671 w	671 vw	670 vw, sh	670 w	670 mw	ν(C−STe)
[*e*]	[*e*]	[672 (20)]	[672 (30)]	[669 (20)]	
	697 mw				
	[697 (5)]				
520 mw, br	535 w, sh	525 vw	535 vw	530 sh	ν(Te−C)$_{asym}$
[527 (55)]	[539 (70)]	[531 (80)]	[536 (80)]	[532 (50)]	
520 mw, br	515 w, sh	514 w	520 vw	520 sh	ν(Te−C)$_{sym}$
[519 (100)]	[514 (100)]	[518 100)]	[519 (100)]	[518 (60)]	
330 s, br	315 vs, br	359 m	368 m	365 ms	ν(Te−S)[f]
[345 (80)]	[350 (60)]	[356 (40)]	[367 (80)]	[360 (100)]	
		208 s	138 m	107 mw	ν(Te−X)[g]

[a] Run neat between KBr plates down to 400 cm^{-1} and between polyethylene below 400 cm^{-1}. [b] Run neat in sealed capillaries. [c] Parentheses denote relative intensities in the Raman effect. [d] s = strong, m = medium, w = weak, sh = shoulder, br = broad, and v = very. [e] Not observed. [f] Both asymmetric and symmetric stretches are present in **1**, **2**, and **3**. [g] Quality of Raman spectra very poor below 200 cm^{-1}. [h] Overlap of the bands in the two ligands.

C−S and S−C−N angles in all eight molecules are essentially the same at 122(2)°, consistent with the π-bond delocalization within the S_2CN planar moiety being greater and approximately of equal importance in the S_2C−N and TeS(N)C−S bonds. The (Te)S−C bonds, which average 1.75(3) Å, are typical of the S−C bond attached to the stronger Te−S bond in anisobidentate dithiocarbamate and monothiocarbamate derivatives[17] and also shorter than the sum of the covalent radii of C and S of 1.81 Å, suggesting a small degree of participation in the delocalized π-bonding. The C−S bond, involving the terminal or weakly bonded sulfur atom, has an average length of 1.67(3) Å in these and other dithiocarbamates. It is considerably shorter than the nominally single C−S bond, longer than the C═S bond, which typically is close to 1.56 Å in CS_2, COS, or CSTe,[33] but similar to the bond length observed in species such as $(NH_2)_2CS$, and thus consistent with a considerable degree of partial π-bond character as well as an anisobidentate link. The average S_2C−N bond length of 1.33(2) Å is similar to those reported for other dithiocarbamates and related monothiocarbamates and considerably shorter than the sum of the covalent radii of C and N of 1.51 Å, confirming that π-electron delocalization is extending to the S_2C−N bond.

The sum of the three angles about N of 360° confirms that the nitrogen atom is also planar. The two SC−N−C angles have an average value of 124(2)°, and the average C−N−C angle for the carbon atoms in the ring is 112(3)°, consistent with the π-bonding being extensively involved with the S_2C−N bond. The restriction to rotation about the S_2C−N bond is discussed in the section on NMR spectroscopy. Figures 2, part b, 3, part b, 5, 7, and 8 clearly show the preferred chair form of the six-membered ring in the piperidyl complexes, and in all complexes the atoms in the rings furthest from nitrogen generally show the largest thermal parameters, as is to be expected.

Infrared and Raman Spectra. Characteristic features of the infrared and Raman spectra of compounds **1−9** are summarized in Table 18. The assignments are primarily based on those reported for *N*,*N*-dialkyl dithiocarbamate derivatives in general and tellurium derivatives in particular,[10,15] along with those on the related pyrrolidyl and piperidyl monothioformate derivatives of tellurium.[17] It has been claimed for some time that the characteristic (C−NR_2) stretching vibration is generally seen in the range 1450−1550 cm^{-1} where, in the presence of CH_n groups, it is assigned in the infrared spectrum to the peak which has significantly higher intensity than those associated with the CH_n deformation modes and which is usually at highest wavenumber within the specified region. The position reflects the fact that ν(C−NR_2) frequencies are much closer to those expected for a C═N double bond (approximately 1600 cm^{-1} for a bond length of 1.27 Å) than for a C−N single bond (approximately 1000 cm^{-1} for a bond length of 1.46 Å), reflecting the significant π-character of the bond. In all of the pyrrolidyl complexes there is such a peak assignable to ν(C−NR_2) in the region 1432−1444 cm^{-1}, which is at slightly lower wavenumber than those generally observed in the dialkyl

(33) Wells, A. F. *Structural Inorganic Chemistry*, 4th ed; Clarendon Press: Oxford, 1975; p 739.

Table 19. $^{13}C\{H\}$ NMR Chemical Shifts for the Dimethyl- and Halodimethyltellurium Pyrrolidyl and Piperidyl Dithioformates **1**−**9**[a]

no.	compd	Te-*C*H_3	S-*C*	N−*C*	NC-*C*
1	$Me_2Te[S_2CN(CH_2)_3CH_2]_2$	16.46	195.01	53.73	26.00
2	$Me_2Te[S_2CN(CH_2)_4CH_2]_2$	17.03	198.52	52.34	25.94
3	$Me_2Te[S_2CN(CH_2)_3CH_2][S_2CN(CH_2)_4CH_2]$	16.75	195.90	53.75	26.00
			198.40	52.34	25.94
4	$Me_2TeCl[S_2CN(CH_2)_3CH_2]$	20.43	191.20	54.09	26.04
5	$Me_2TeBr[S_2CN(CH_2)_3CH_2]$	19.66	190.80	54.26	26.10
6	$Me_2TeI[S_2CN(CH_2)_3CH_2]$	18.18	191.22	54.37	26.15
7	$Me_2TeCl[S_2CN(CH_2)_4CH_2]$	20.69	193.31	52.98	25.90
8	$Me_2TeBr[S_2CN(CH_2)_4CH_2]$	19.95	192.34	53.12	25.93
9	$Me_2TeI[S_2CN(CH_2)_4CH_2]$	18.41	192.83	53.18	25.97

[a] The spectra were recorded in $CDCl_3$ and reported in ppm from Me_4Si. [b] Peaks attributable to NCC−*C* seen at 24.13 (**2**), 24.12 (**3**), 23.74 (**7**), 23.69 (**8**), and 23.68 (**9**).

derivatives. In the piperidyl complexes, and indeed the starting salt $NaS_2CN(CH_2)_4CH_2$, two intense peaks appear in all cases between 1468−1481 and 1422−1435 cm^{-1}, which are generally significantly more intense than peaks attributable to the six-membered ring or the hydrogen atoms attached to it. In neat piperidine, there is a peak at 1443 cm^{-1}, so it is possible that the two peaks in the dithiocarbamate arise from the Fermi resonance between ν(C−NR_2) and $\delta(CH_2)$. The C−N bond lengths are essentially the same in both sets of derivatives and similar to those in other $R'_2Te[S_2CNMe_2]_2$ and $R'_2Te[S_2CNEt_2]_2$ species, where ν(C−NR_2) was assigned in the region 1490−1519 cm^{-1}.[10,15] Thus, the variations probably arise from differences in the mixing of the modes in the planar moieties and possibly the greater effective mass of the rings, rather than differences in the strength of the C−N bond.

The conventional assignment of the C−S(terminal) stretching vibration in dithiocarbamates is in the 980 cm^{-1} region and in a series of $R_2Te[S_2CNR'_2]_2$ and $R_2TeCl[S_2CNR'_2]$ derivatives, where R = Me, $MeOC_6H_4$ and R′ = Me, Et;[15] the assignment was made in the range 963−982 cm^{-1}. The corresponding peak appears at 942−949 cm^{-1} for the pyrrolidyl derivatives and 961−972 cm^{-1} for the piperidyl. Conversely, although ill-defined, the C−STe stretching vibrations appear to be at a slightly higher wavenumber for the pyrrolidyl derivatives at *ca.* 695 cm^{-1} than for the piperidyl at *ca.* 670 cm^{-1}, these being typical locations for a C−S single bond, similar to the values observed in the monothiocarbamate species,[17] and consistent with the bond lengths in **1**, **2**, **3**, **4**, **5**, **6**, **7**, and **9** being close to the sum of the covalent radii of C and S. The assignment between 942 and 972 cm^{-1} still places the C−S(terminal) vibrations in a region between the weighted average of ν(C−S) in the partially double-bonded C−S bond in the CS_3^{2-} ion which is *ca.* 800 cm^{-1},[34] and closer to the average value in CS_2 of 1090 cm^{-1}. As noted in the discussions on the structures, the terminal C−S distances are similar in all derivatives, averaging 1.67(3) Å which is consistent with partial π-bond character, and shorter than the C−STe bonds which are closer to the sum of the covalent radii. The slight difference between the series in the assignments of the two modes is probably a reflection of different degrees of mixing of the modes. The general similarity of the location and appearance of the bands in all nine compounds is consistent with the dithiocarbamate groups being attached in the same, essentially anisobidentate, fashion as observed in all of the crystal structures of the tellurium derivatives. By analogy with the Me_2TeX_2 series, where X = Cl, Br, and I,[35] and the monothiocarbamate series, where X = $SCONR_2$, Cl, Br, and I,[17] the asymmetric and symmetric Te−C stretching vibrations are readily assigned to prominent peaks in close proximity in the Raman spectra in the region between 539 and 514 cm^{-1}. The corresponding peaks are very weak in the infrared spectrum. The small split between the symmetric and asymmetric modes is consistent with a C−Te−C angle close to 90°, and the similarity in all positions is consistent with the lack of variation in the Te−C bond lengths. The Te−S stretching vibration in the halodithiocarbamate derivatives, **4**−**9**, is assigned to peaks which are medium to strong peaks in both the Raman and in the far-infrared spectra in the range 335−368 cm^{-1}, which appears to be a fairly broad range given that the Te−S bond lengths in **4**, **5**, **6**, **7**, and **9** are all close to the average value of 2.51(2) Å. However, in the series $Me_2TeX[S_2COR]$, X = Cl, Br, and I and R = Me, Et, and *i*-Pr, where the assignments were supported in part by normal coordinate analysis;[37] ν(Te−S) was assigned within an even broader range, 318−379 cm^{-1}, even though the two structures that were solved indicated identical Te−S bond lengths (2.518(3) Å for X = Cl and R = Me and 2.517(3) Å for X = I and R = *i*-Pr). In the fully substituted species, **1**−**3**, the corresponding peaks in the infrared and Raman spectra do not coincide, as is to be expected because both asymmetric and symmetric Te−S stretching modes are now present. The average value for these modes (331 cm^{-1}) is less than that in the halogenated derivatives (355 cm^{-1}), which is at least consistent with the longer Te−S bonds (average 2.62(2) Å) in the solid state structures of **1**−**3**.

Because the vibrational spectra consistently gave a general shift to lower wavenumber for ν(Te−S) as the Te−S bond length increased and hence presumably weakened, a similar phenomenon might be confirmed for the Te−X stretching vibrations in **4**−**9**, as it was in the $Me_2TeX[S_2CNEt_2]$ and $Me_2TeX[S_2COR]$ series.[17,37] The crystal structures of **4**, **5**, **6**, **7**, and **9** all indicate that the Te−X bonds are longer, and presumably weaker, than those in Me_2TeX_2, in which the average values for the symmetric and asymmetric Te−X stretches are 264, 169, and 129 cm^{-1}, respectively, for X = Cl, Br, and I. Unfortunately, we were not able to obtain Raman spectra of good quality below *ca.* 200 cm^{-1} and so have to rely on the rather broad and somewhat ill-defined far-infrared spectra. Nevertheless, for **4**−**9**, there are peaks assignable to ν(Te−X) at 208 cm^{-1} for **4** and **7**, where X = Cl, at 137 and 138 cm^{-1} for **5** and **8**, where X = Br, and at 108 and 107 cm^{-1} for **6** and **9**, where X = I, consistent with the presence of a Te−X bond significantly longer than that in the Me_2TeX_2 species, and the assignments are in agreement with those made for the $Me_2TeX[SCON(CH_2)_3CH_2]$ and $Me_2TeX[S_2COR]$ derivatives.[17,37]

$^{13}C\{H\}$ NMR Spectra. The ^{13}C NMR spectral data for compounds **1**−**9** are displayed in Table 19. In $Me_2Te[S_2CN(CH_2)_3CH_2]_2$ **(1)** there are four sets of peaks, all singlets, at 195.01 (S_2CN), 53.73 (NCH_2), 26.00 ($NCCH_2$), and 16.46 (CH_3) ppm. This is in marked contrast to the spectrum of the

(34) Ross, S. D. *Inorganic IR and Raman Spectra*; McGraw Hill: London, 1972; p 160.
(35) Hayward, G. C.; Hendra, P. J. *J. Chem. Soc. A* **1969**, 1760.

Table 20. ^{1}H and ^{125}Te NMR Chemical Shifts for the Dimethyl- and Halodimethyltellurium Piperidyl and Pyrollidyl Dithioformates **1**−**9**[a,b]

no.	compd	Te−CH_3[c]	N−CH_2	NC−CH_2	^{125}Te
1	$Me_2Te[S_2CN(CH_2)_3CH_2]_2$	2.49 (6H)	3.76 (8H)	2.00 (8H)	500.1
2	$Me_2Te[S_2CN(CH_2)_4CH_2]_2$	2.48 (6H)	4.11 (8H)	1.65 (12H)[d]	464.7
3	$Me_2Te[S_2CN(CH_2)_3CH_2][S_2CN(CH_2)_4CH_2]$	2.49 (6H)	3.76 (4H)	2.00 (4H)	469.5
			4.11 (4H)	1.66 (6H)[d]	
4	$Me_2TeCl[S_2CN(CH_2)_3CH_2]$	2.77 (6H)	3.72 (4H)	2.05 (4H)	552.4
5	$Me_2TeBr[S_2CN(CH_2)_3CH_2]$	2.79 (6H)	3.73 (4H)	2.06 (4H)	534.3
6	$Me_2TeI[S_2CN(CH_2)_3CH_2]$	2.80 (6H)	3.73 (4H)	2.05 (4H)	507.5
7	$Me_2TeCl[S_2CN(CH_2)_4CH_2]$	2.77 (6H)	4.03 (4H)	1.69 (6H)[d]	547.5
8	$Me_2TeBr[S_2CN(CH_2)_4CH_2]$	2.79 (6H)	4.02 (4H)	1.69 (6H)[d]	528.5
9	$Me_2TeI[S_2CN(CH_2)_4CH_2]_2$	2.81 (6H)	4.04 (4H)	1.69 (6H)[d]	501.0

[a] The spectra were recorded in $CDCl_3$ and reported in ppm from Me_4Si for ^{1}H and from Me_2Te for ^{125}Te. [b] Number of protons are in parentheses. [c] In all compounds, the value of J(HTe) is within the range 25−27 Hz. [d] Includes overlapping peaks arising from NCCCH_2.

corresponding monothiocarbamate, $Me_2Te[SCON(CH_2)_3CH_2]_2$,[17] in which there are also four sets of peaks with singlets at 170.29 (S*C*ON) and 14.72 (Te*C*H_3), but with doublets at 46.61 and 48.57 (N*C*H_2) and at 25.06 and 25.57 (NC*C*H_2) ppm. The same nonequivalence was observed for the halo-substituted monothiocarbamate derivatives, but only single peaks are seen in the halo-substituted pyrrolidyl and piperidyl derivatives, **4**−**9**, and in **2** and **3**, as was previously noted for the alkyl groups in (*N*,*N*-dialkyl dithiocarbamato)tellurium derivatives.[15] The presence of two sets of peaks of equal intensity assignable to the ring carbon atoms for the monothiocarbamate, but not for the dithiocarbamates derivatives, is an indication that the former maintain essentially monodentate ligands in solution, while the latter show behavior more consistent with the presence of bidentate ligands. The unsymmetrical bidentate (or anisobidentate) ligands seen in the solid state structures of **1**, **2**, **3**, **4**, **5**, **6**, **7**, and **9** could be expected to undergo rapid equilibrium in solution. The values of the chemical shifts for the single peak of the N−*C* and NC−*C* carbon atoms are very similar regardless of whether they are part of a five-membered or six-membered ring as emphasized by the mixed ligand species, **3**, with values of 53.75 and 52.34 ppm for N−*C* and of 26.00 and 25.94 ppm for NC−*C* in the pyrrolidyl and piperidyl rings, respectively. Thus, the similarity of environment in both groups is illustrated. The chemical shifts of the methyl groups attached to tellurium are similar in compounds **1**−**3**. The Te−CH_3 chemical shift of the mixed ligand species, at 16.75, is between that of **1** and **2** and confirms that this is a mixed ligand species rather than a mixture of the two bis compounds. The values are essentially the same as those of the $Me_2Te[S_2CNR_2]_2$ species, R = alkyl, and between those of the $Me_2Te[SCONR_2]_2$ species (*ca.* 14.8 ppm) and those of the $Me_2Te[S_2POGO]_2$ series (*ca.* 19.2 ppm).[36] The slight upfield shift as the electronegativity of the halogen substituent decreases for the two series **4**−**6** and **7**−**9** is consistent with the observation that the starting materials Me_2TeCl_2, Me_2TeBr_2, and Me_2TeI_2 have chemical shifts of 26.9, 25.1, and 22.0 ppm, respectively. The similarity in the values of the Te−*C*H_3 chemical shifts of the halo(pyrrolidyl and piperidyl) compounds again suggests similar environments for all of these compounds in solution. The S_2CN chemical shifts are also similar for all nine compounds, consistent with similar environments around the planar C atom. The pyrrolidyl compounds consistently have slightly lower values than their piperidyl counterparts, with **3** clearly showing peaks both at 195.90 ppm (pyrrolidyl ligand) and 198.40 ppm (piperidyl ligand). The halogen derivatives (**4**−**9**) have slightly lower values (*ca*. 191 and 193 ppm for the pyrrolidyl and piperidyl derivatives, respectively) than the bis compounds as was noted for the monothiocarbamate derivatives with values of *ca*. 170 ppm for the bis compounds and *ca*. 166 ppm for the series $Me_2TeX[SCON(CH_2)_3CH_2]$. Analogous dithiocarbonate compounds have values in the range 215−218 ppm for $Me_2TeX[S_2COR]$ species.[37]

^{125}Te NMR Spectra. The ^{125}Te NMR spectral data for compounds **1**−**9** are presented in Table 20. All compounds give a single peak consistent with the presence in solution of one compound containing tellurium. In $Me_2Te[S_2CNMe_2]_2$ and $Me_2Te[S_2CNEt_2]_2$, the peak is seen at 475 and 463 ppm, the latter being very close to the value of 464.7 ppm found in $Me_2Te[S_2CN(CH_2)_4CH_2]_2$ **(2)**. Although the value of 469.5 ppm in **3** is between that of **2** and **1** (500.1 ppm), it is certainly not at the average value. For both series of partially substituted halo derivatives, the values are higher than those of the bis compounds, 552.4, 534.3, and 507.5 ppm for **4**−**6** and 547.5, 528.5, and 501.0 ppm for **7**−**9**. The values for the pyrrolidyl derivatives, **4**−**6**, are remarkably similar to those of the corresponding monothiocarbamate series, $Me_2TeX[S_2CN(CH_2)_3CH_2]$, where the values are 554, 536, and 516 ppm, respectively, for X = Cl, Br, and I. The chemical shifts of these chloro and bromo derivatives are much closer to the values for the bis compounds than to those for the dihalide starting materials, Me_2TeCl_2 (733.8 ppm) and Me_2TeBr_2 (649.2 ppm). This suggests that the thio groups have much more influence on the environment about tellurium than do the halogens, which is consistent with the unusually long Te−X bonds found in the solid state structures of these halo derivatives being maintained in solution.

^{1}H NMR Spectra. The ^{1}H NMR spectral data for compounds **1**−**9** are summarized in Table 20. All the derivatives show a sharp singlet assignable to the methyl group attached to tellurium, and the CH_3−Te chemical shift of *ca.* 2.49 ppm for **1**−**3** is essentially the same as that found for the $Me_2Te[S_2CNR_2]_2$ species[15] and only marginally higher than that for the $Me_2Te[SCONR_2]_2$ species.[17] In the Me_2TeXL derivatives, **4**−**9**, these singlets are seen in a narrow range from 2.77 to 2.81 ppm. There is a small but consistent downfield shift from Cl to I, which is similar to that between Me_2TeCl_2 (3.10 ppm) and Me_2TeI_2 (3.27 ppm) and has been observed in the previous studies on related halo(di- and monothioformato)tellurium derivatives. Satellite peaks arising from H−Te coupling are observed with the value of the coupling constants being consistently *ca.* 26 Hz.

The peaks attributable to the protons of the rings are seen as single peaks, indicating equivalence of protons attached to the carbon atoms in the same ring position at room temperature. This is at least consistent with all probable processes, anisobidentate to bidentate interconversion, rotation about the C−N partial double bond, and ring motions such as boat−chair−boat

(36) Drake, J. E.; Khasrou, L. N.; Mislankar, A. G.; Ratnani, R. *Can. J. Chem.* **1994**, *72*, 1328.

(37) Drake, J. E.; Drake, R. J.; Khasrou, L. N.; Ratnani, R. *Inorg. Chem.* **1996**, *35*, 2831.

interconversion for the piperidyl derivatives, being rapid on the NMR time scale. The spectra of the pyrrolidyl compounds generally show some fine structure which is consistent with second-order spectra and in fact is essentially identical to that observed in pyrrolidine itself. For $Me_2Te[S_2CN(CH_3)_3CH_2]_2$ **(1)**, two peaks of equal intensity, attributable to NCH_2 and $NCCH_2$, are seen centered at 3.76 and 2.00 ppm, respectively. The corresponding peaks in $Me_2TeX[S_2CN(CH_3)_3CH_2]$ **(4**−**6)** are seen at *ca.* 3.73 and 2.05 ppm, showing essentially the same complex fine structure as **1**.

In the spectra of the piperidyl complexes, **2** and **7**−**9**, the peaks arising from the ring protons are broad, with no fine structure, but again have the expected relative intensities consistent with their formulation. Thus, in $Me_2Te[S_2CN(CH_2)_4CH_2]_2$ **(2)**, two broad peaks are observed at 4.11 (NCH_2) and 1.65 ppm ($NCCH_2$ and $NCCCH_2$ overlapping) with relative intensities of 4:6. The corresponding peaks in $Me_2TeX[S_2CN(CH_2)_4CH_2]$ **(7**−**9)** are at *ca.* 4.03 and 1.69 ppm, with the slight chemical shifts resulting from the presence of the halogen being of the same magnitude and in the same direction as in the pyrrolidyl series. The spectrum of **3** is exactly as expected on the basis of the mixed ligands that are present.

Variable temperature ^1H NMR spectra were recorded in toluene for **1** and **2**. The chemical shifts in toluene are slightly different from those in $CDCl_3$. In **1**, the overall appearance of the spectrum at room temperature is unaltered, whereas in **2**, the peak attributable to $NCCCH_2$ is now seen as a distinct shoulder. In the low-temperature spectra of $Me_2Te[S_2CN(CH_2)_3CH_2]_2$ **(1)** and $Me_2Te[S_2CN(CH_2)_4CH_2]_2$ **(2)** (Figure 11, parts A and B) the only peaks showing significant changes other than some broadening are those attributable to the NCH_2 protons at 3.76 and 4.11 ppm, respectively. These also broaden but then separate into two peaks of equal intensity with a coalescence temperature of *ca.* 190 K. This gives an energy barrier of *ca.* 8.9 kcal mol^{-1} for both molecules; the similarity and value suggest that this probably corresponds to the barrier to rotation about the C−N bond. There were no significant changes in the spectra on heating the molecules so that they are clearly much less susceptible to reductive elimination than the dithiocarbonate analogues reported recently.[2,37]

Thus, these pyrrolidyl and piperidyl dithioformates represent a thoroughly characterized series of organotellurium(IV) derivatives which provide examples of supramolecular associations in the solid state leading to extended structures that involve halogen or sulfur bridges. The resulting unusual stereochemistry of tellurium leads to dimers or pseudopolymers. In solution it appears that the sulfur atoms of the unsymmetrical bidentate ligands observed in the crystal structures undergo rapid exchange, but the derivatives do not readily undergo the facile reductive-elimination that is typical of related tellurium(IV) derivatives.

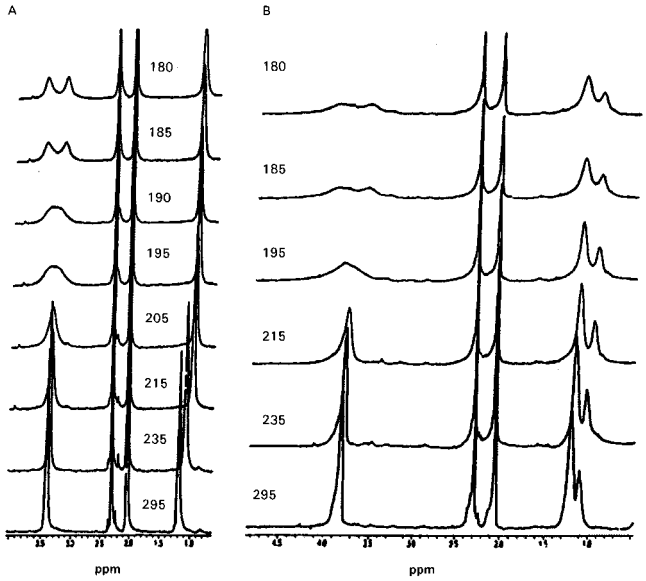

Figure 11. VT ^1H NMR spectrum of (A) $Me_2Te[S_2CN(CH_2)_3CH_2]_2$ **(1)** and (B) $Me_2Te[S_2CN(CH_2)_4CH_2]_2$ **(2)** recorded in toluene between 295 and 180 K.

Acknowledgment. We thank the Natural Sciences and Engineering Research Council of Canada for financial support.

Supporting Information Available: Tables S.1−S.13, listing experimental details, anisotropic thermal parameters for non-hydrogen atoms, and final fractional coordinates and thermal parameters for hydrogen atoms (19 pages). Ordering information is given on any current masthead page. Structure factor tables may be obtained directly from the authors.

IC9608455